Chapter 1

Introduction

In acoustics, as in almost any analytical field, the traditional approach to solving a problem is to describe it in the form of an equation and then to linearize this equation. In kinematic terms this means that the motion of the oscillating system is assumed to be small when compared to its structural dimensions. The unknown quantity whether it is displacement, velocity or pressure need only be included in the equation of motion if it is of first order; higher order terms are considered negligible. The consequences of this seemingly small assumption are far-reaching and, together with a range of techniques developed to solve the linear equations, they account for most of our present knowledge in acoustics.

Amongst the predicted phenomena of linear theory, the two most telling are probably that the frequency of oscillation of a system is independent of the amplitude and, the existence of modes of vibration such that each mode is independent of any other mode so that the total vibration is a linear superposition of the individual modes that may at any stage be separated into its constituent parts.

Thus it is quite obvious that for some problems, for example a string plucked with large amplitude such that its frequency decreases as its amplitude decays, the linear approach is insufficient. It was this very problem that prompted the first detailed investigation into the theory of nonlinear vibrations of elastic structures (Carrier 1945), a paper we shall examine in more detail in chapter 2. Carrier's paper is typical of most of the work done on nonlinear problems up till very recently, that is, having realised the problem is not linear so that all the elegant techniques for solving linear equations of motion are not in the main, helpful, the investigator needs to develop new methods of solution. This is done by assuming the system responds with a particular, simple solution and then iterating successively until the

solution converges to a reasonable approximation of the actual response.

For example one common method, the perturbation method, expands an assumed solution in terms of the nonlinear parameter so that accuracy may be increased simply by inclusion of higher order terms from the expansion. A trial solution is taken from the linearized problem and then substituted into the equation with as many of the nonlinear expansion terms present as necessary to obtain an adequate approximation to the actual response. Another method, the method of slowly varying parameters, we shall be using in chapters 3 and 5. It has an advantage in that it enables us to determine not only the steady-state periodic motions but also the transient process corresponding to the perturbations of the oscillations. The method is used with equations of the form

$$\ddot{x} + \omega^2 x + g(x, \dot{x}) = 0 \tag{1.1}$$

where $g(x, \dot{x})$ is weakly nonlinear.

We know that if $g(x, \dot{x}) = 0$ then (1.1) reduces to

$$\ddot{x} + \omega^2 x = 0 \tag{1.2}$$

the solution of which is just

$$x = a\sin(\omega t + \phi) \tag{1.3}$$

where a and ϕ are constants and

$$\frac{dx}{dt} = a\omega\cos(\omega t + \phi). \tag{1.4}$$

Now if $g(x, \dot{x})$ is sufficiently small we may assume that the solution to (1.1) will be of the form

$$x = a(t)\sin(\omega t + \phi(t)) \tag{1.5}$$

where a and ϕ are functions of t, to be determined such that the derivative of (1.5) is of the same form as (1.4)

$$\frac{dx}{dt} = a(t)\omega\cos(\omega t + \phi(t)). \tag{1.6}$$

Substitution of (1.5), (1.6) and the second derivative of x, obtained by differentiating (1.6) with respect to time, then gives us the equations

$$\frac{da}{dt} = -\frac{g(x, \dot{x})}{\omega}\sin(\omega t + \phi) \tag{1.7}$$

$$\frac{d\phi}{dt} = -\frac{g(x, \dot{x})}{a\omega}\cos(\omega t + \phi) \quad . \tag{1.8}$$

These equations are exact for the functions $a(t)$ and $\phi(t)$ when the solution of (1.1) is of the form (1.5), but they themselves are still difficult to solve. We therefore assume that the the nonlinearity and rate of change are both small so that $a(t)$ and $\phi(t)$ change only slowly over one cycle. Thus if we calculate the average values of a and ϕ over one period, (1.7) and (1.8) may be written as

$$\langle \dot{a} \rangle = \langle -\frac{1}{2\pi\omega} \int_0^{2\pi} g(a\sin\theta, a\omega\cos\theta)\cos\theta\, d\theta \rangle \tag{1.9}$$

$$\langle \dot{\theta} \rangle = \langle \frac{1}{2\pi\omega} \int_0^{2\pi} g(a\sin\theta, a\omega\cos\theta)\sin\theta\, d\theta \rangle \tag{1.10}$$

where $\theta = \omega t + \phi$ and the brackets $\langle\rangle$ indicate that only terms with near zero frequency should be retained.

With the increase in interest in nonlinear problems and the development of high powered electronic computers enabling numerical solutions, it is becoming relatively straightforward, though by no means simple, to include nonlinear terms in equations of motion and to choose an appropriate method of solution. In chapters 3 and 5 we shall be solving such problems for a string and a bar respectively and shall show the calculated results approximate well to the experimentally obtained responses.

Yet there are systems for which these methods appear to fail. The equations of motion may be completely determined with no random parameters and still the output appears random. Such systems are said to be chaotic and have recently generated a great deal of interest not only with mathematicians who first started exploring the ideas but also with engineers and physicists who are realising that many physical systems in nature, hereto described as random may actually be chaotic. It is interesting to note too, that if certain parameters are changed by a small amount the chaos may disappear and the response becomes periodic. A good introduction to chaos is contained in a work by Crutchfield, Farmer, Packard and Shaw (1986).

One of the earliest reported chaotic systems was discovered by Lorenz (1963; see also Tongue 1985). In his investigations into atmospheric turbulence, Lorenz studied equations of the form

$$\dot{x} = -\sigma x + \sigma y \tag{1.11}$$

$$\dot{y} = -xz + rx - y \tag{1.12}$$

$$\dot{z} = xy \tag{1.13}$$

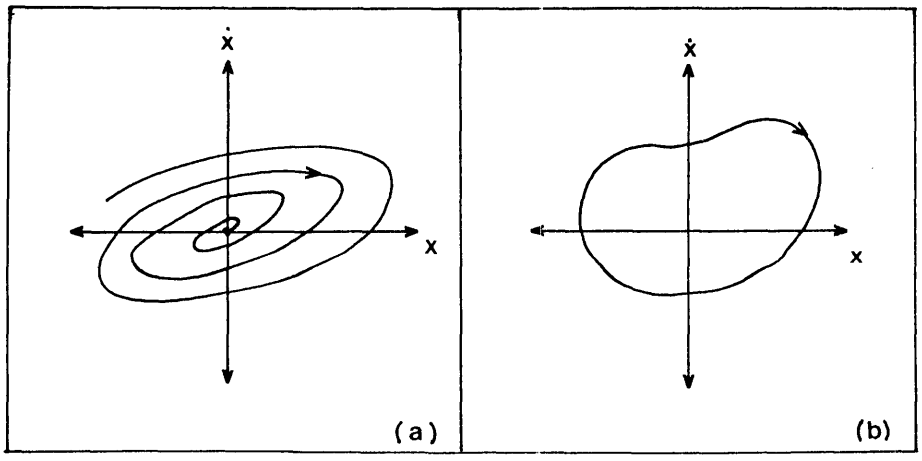

Figure 1.1: Phase Space flow of (a) a system that comes to rest under the influence of friction and (b) a system that cycles periodically without coming to rest.

for which he found that suitable values of σ and r would cause the system to respond chaotically.

Chaotic systems are best depicted in phase space where the coordinates are usually velocity and position. The system's state can then be illustrated as it changes in time; either continuously, called a flow, or at discrete time intervals, called a mapping. For example, a system that comes to rest under the influence of friction, will have a flow that approaches a single point, called an attractor (Fig.1.1a). Systems that do not come to rest but cycle periodically, have flows represented by closed orbits called limit cycles, (Fig. 1.1b). A Poincare mapping of such a system, where the state of the system is measured at discrete time intervals equal to the period of the motion, will obviously be a single point. Some systems have two or more possible modes of vibration so that their attractor depends on the initial conditions of the system.

Slightly more complicated systems such as those with quasi-periodic motion where, for instance, the system may be being driven at a frequency slightly off its normal resonant frequency, display torus shaped attractors. Despite their seemingly complicated behaviour such systems are still predictable in their motion.

Chaotic systems have what are known as "strange attractors ", that is, their response is a bounded oscillation containing a continuum of frequencies so that a Poincare mapping will contain a seemingly random array of points within an infinitely detailed surface (Fig.1.2).

Figure 1.2: A strange attractor calculated by the author using the equation $\ddot{x} + 0.02\dot{x} + x(1 + 0.3x + 0.1x^2) = 25\sin t$.

Furthermore two points infinitely close on the strange attractor may strongly diverge within a few cycles, illustrating the unpredictable nature of chaotic motion.

With this in mind Holmes (1979) identified Lorenz's findings as a strange attractor along with similar types of results obtained in studies of population dynamics, fluid dynamics and models of the earths magnetic field. He has written a thorough and fairly mathematical study into chaos as found for the Duffing oscillator

$$\ddot{x} - k\dot{x} - \beta x + \alpha x^3 = F\cos(\omega t) \tag{1.14}$$

in which he shows not only its chaotic behaviour for a range of values of F, but also establishes Poincare mapping as a suitable means by which to study chaos.

Ueda (1979) investigates the transition of a system from periodic motion to chaotic motion. He uses a particular Duffing oscillator given by the equation

$$\ddot{x} + k\dot{x} + x^3 = F\cos t \tag{1.15}$$

and records the Poincare mapping and power spectrum as the parameters k and F are varied. Ueda concludes that the road to chaos is through multiple frequency splitting (period doubling, tripling, etc.) as a critical parameter is changed. That is, for a given

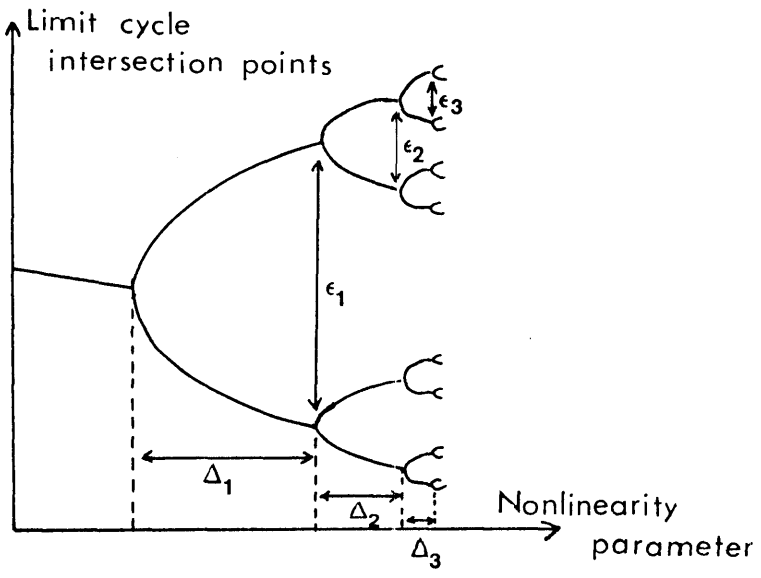

Figure 1.3: Bifurcation Tree showing universal behaviour in the road to chaos.

force and decay rate, a system may display periodic motion with a period of T . If the force is then increased (or the decay rate decreased) to a particular value the motion will bifurcate so that it oscillates with, say, twice the period, 2T . If the force is increased still further there comes a point where the period again bifurcates so that it is now 4T before the motion repeats itself. If the force is increased past a critical value there comes a point where the period is 2^{∞}T so that the motion although still bounded never repeats itself. This is chaos.

A major breakthrough in the understanding of chaos came when Feigenbaum (1980) discovered universal behaviour in the road to chaos. If we represent the road as a "bifurcation tree" which is simply a graph of how the limit cycle in phase space splits up as bifurcations occur, then two numbers become apparent (Fig.1.3), such that, for large values of i,

$$\frac{\Delta_i}{\Delta_{i+1}} - \delta = 4.6692 \tag{1.16}$$

and

$$\frac{\epsilon_i}{\epsilon_{i+1}} \rightarrow \alpha = 2.5029 \ . \tag{1.17}$$

These numbers are the same for almost all chaotic systems and have since been measured in a variety of experiments.

The reason why a particular system may become chaotic, however, is yet to be determined. It has been suggested (Holmes and Moon,1983) that the existence of both stable and

unstable equilibrium states for a system may be a necessity for chaotic behaviour. Thus for small forcing terms the motion may take place within a potential well and will be periodic. If the force is increased however, it may become large enough to make the system jump from one equilibrium point to another. This rather elegant conjecture was soon disproved by Tongue (1985) with the example

$$\ddot{x} + 0.1\dot{x} + x^3 = F\cos(\omega t) \tag{1.18}$$

which has only one stable equilibrium point at the origin and no unstable equilibria yet still displays chaotic behaviour for particular values of F and ω.

There is obviously much work still to be done towards the understanding of chaos itself but there is no doubt that we have now, a powerful new tool with which to investigate nonlinear systems.

In chapter 7 we shall describe the behaviour of the gong in terms of coupled Duffing equations and shall see how this may produce both bifurcations and chaos depending on the forcing and damping terms. Duffing oscillators have been used as examples in the study of chaos (Holmes, 1979; Ueda, 1979; Tongue, 1987), for single mode systems. Most pertinent to our investigations is the study by Tongue(1987) in which the author examines a generalised form of Duffing's equation. In particular, he points out the dangers involved in numerical integrations of equations with insufficient time steps. Fig. 1.4 is a Poincare map as shown by Tongue for the equation

$$\ddot{x} + 0.2\dot{x} - x + x^3 = 0.3\cos(1.2t) \tag{1.19}$$

The small dots depict a strange attractor generated with time steps equal to 0.2618. However, if the time steps are reduced to 0.0654 the Poincare map shows that the response is actually periodic with five points. Still smaller time steps cause no further change in the map. Clearly, we must take particular care with numerical integrations in our search for chaotic motion.

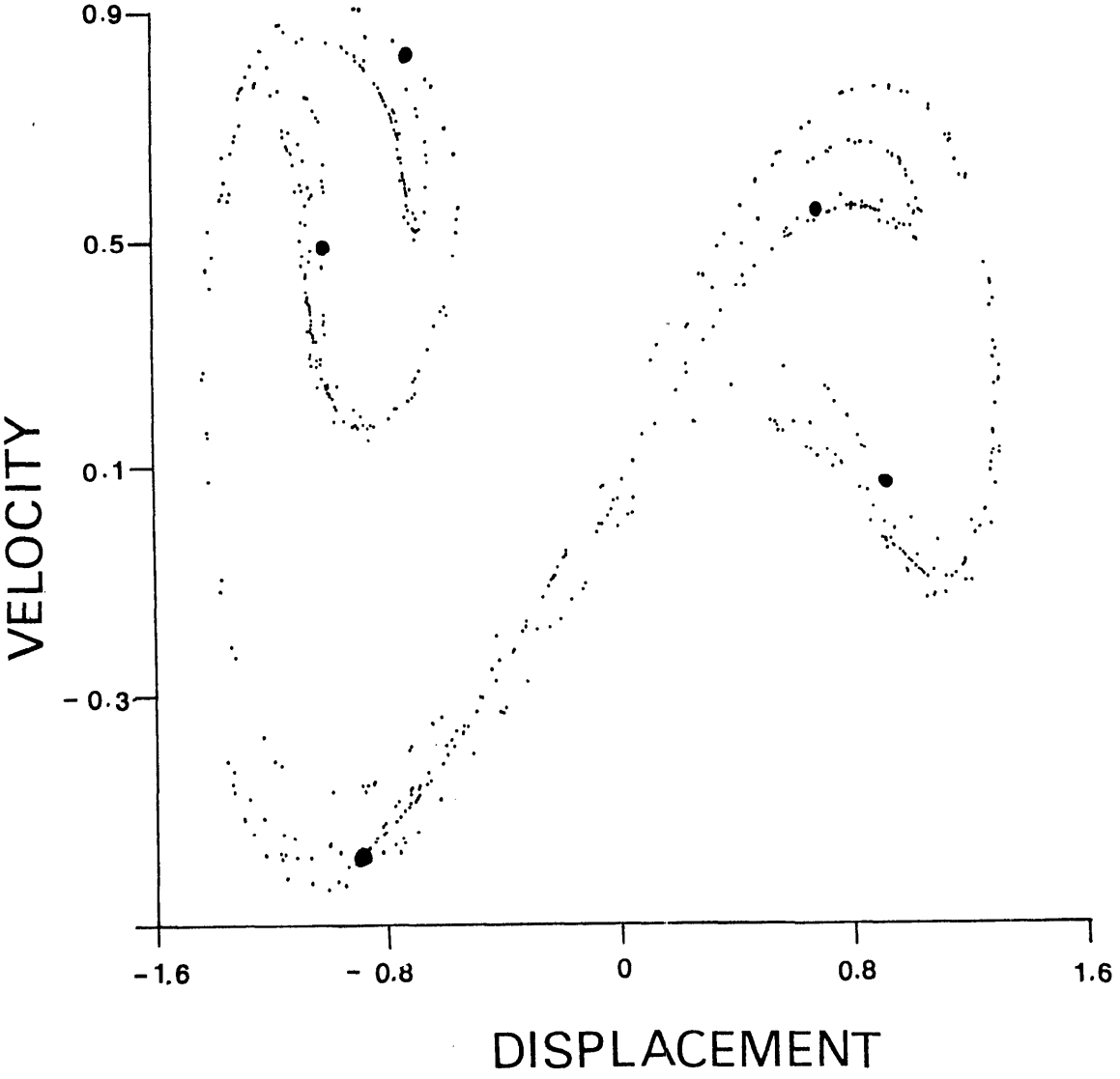

Figure 1.4: Poincare Map of $\ddot{x} + 0.2\dot{x} - x + x^3 = 0.3\cos(1.2t)$. The small and large dots were generated with time steps equal to 0.2618 and 0.0654 respectively indicating that care must be taken to choose small enough time steps when integrating numerically [from Tongue 1987].

GLOSSARY OF SYMBOLS COMMONLY USED IN CHAPTERS 2 AND 3 FOR THE STRING.

x	position along string
t	time
$y(x,t)$	transverse displacement
$z(x,t)$	transverse displacement [normal to y direction]
$v(x,t)$	longitudinal displacement
$u(t)$	temporal component of y(x.t)
$\psi(x,\omega)$	characteristic function
ω	radial frequency
a	amplitude
ϕ	phase angle
θ	$(\omega t + \phi)$
c_t	transverse velocity
c_l	longitudinal velocity
T	tension
T_0	tension in rest position
E	Young's modulus
S	cross-sectional area
ρ	mass per unit length
L	string length
δ	apparent increase in string length
$\Delta\omega$	difference between driving frequency and actual mode frequency
Z_0	characteristic impedance of the string
Y_B	mechanical admittance of the bridge
Z_B	mechanical impedance of the bridge
C	compliance of the bridge
F	force on compliant bridge
D	damping
τ	decay constant (total system)
τ'	decay constant (due to bridge only)
τ''	decay constant (due to viscous and internal losses of the string)
β	mode coupling coefficient

Chapter 2

Review on the Nonlinearity of the String

It is well known from the standard analysis of the motion of stretched strings (Morse 1948) that they can be excited in such a way that particular modes have zero amplitude. Thus for example, for the case of an ideal string stretched between rigid supports, in which situation all the modes are harmonics of the fundamental, the n^{th} harmonic and all its multiples $mn(m = 1, 2, 3....)$ are absent if the string is excited by plucking or striking it at a point $\frac{1}{n}$ of its length from one end.

These conclusions are modified only in detail if the theory is extended to include the stiffness of a real string or the incomplete rigidity of real end supports, both of which make the modes of a real string slightly inharmonic (Morse 1948). It is always possible, according to the standard linear theory, to eliminate a particular mode from the motion by applying the excitation at one of the nodes of that mode or, more generally, in such a distribution that the excitation function is orthogonal to the mode shape function.

It comes as something of a surprise, therefore, to find that in practical cases, for example in musical instruments with plucked or hammered strings, these modes are not actually absent from the motion. Rather, they typically begin with near- zero amplitude, rise to a peak after a time of the order of 0.1 seconds, and then decay.

As we have already mentioned, in a linear system the normal modes are uncoupled and, in the presence of viscous damping forces, each mode will simply decay with its own characteristic lifetime. Clearly then, the phenomena described above can only be a result of nonlinear mechanisms coming into operation.

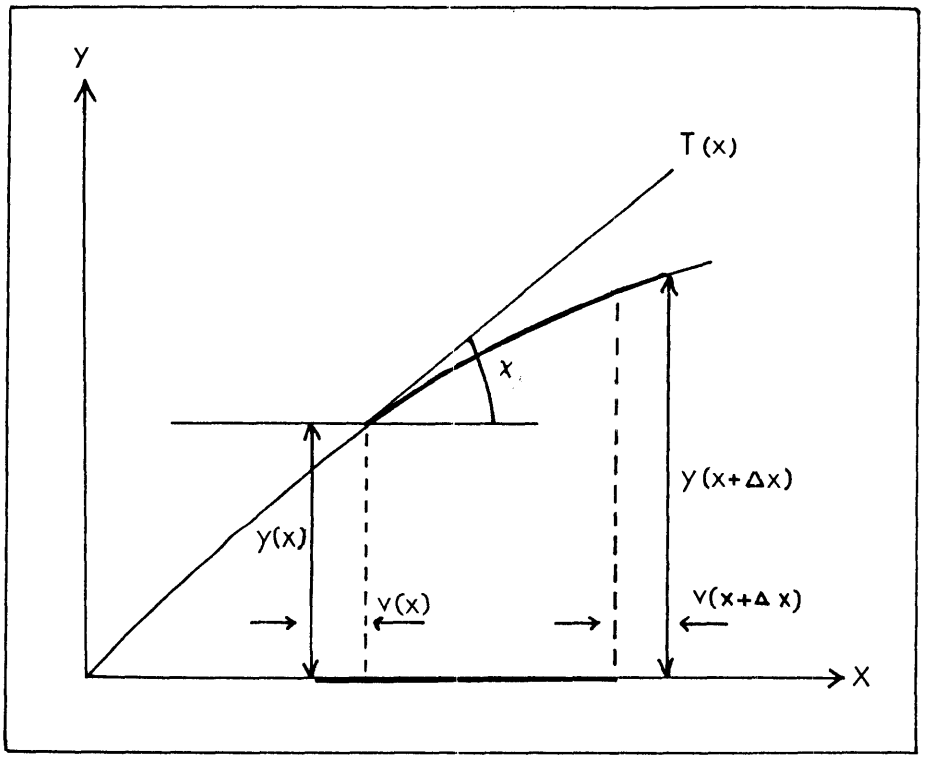

Figure 2.1: Displaced element of string.

Like most other systems, the stretched string is linear to only a first approximation. It has long been recognized that the major cause of nonlinearity is the fact that any small transverse displacement of the string must make a second-order change in its length and therefore in its tension. Such a change in tension may well be negligible in small amplitude vibrations but as linear theory depends on the restoring force being constant for the string, large amplitude vibrations will quite obviously be affected.

Although the basic cause of nonlinearity in string vibrations has been known for a long time, Carrier(1945) appears to have been the first to publish a detailed theoretical analysis. He gives a detailed solution for the free vibration of a string with fixed end supports in which he both derives and solves the equations of motion valid at large amplitudes. In his paper he considers the dynamic equilibrium of an element Δx, of the string, deformed into a plane curve as depicted in Fig. 2.1 such that it undergoes both a transverse displacement $y(x,t)$ and a longitudinal displacement $v(x,t)$. The apparent change in length of the element leads

to a change in tension, written as

$$T - T_0 = ES\left\{\left[\left(1 + \frac{\partial v}{\partial x}\right)^2 + \left(\frac{\partial y}{\partial x}\right)^2\right]^{\frac{1}{2}} - 1\right\} \tag{2.1}$$

where T_0 is the tension in the rest position, E is the Young modulus of the string material and S is the cross-sectional area. The equations of motion in the transverse and longitudinal directions are written

$$\frac{\partial}{\partial x}[T \sin \chi] = \rho \frac{\partial^2 y}{\partial t^2} \tag{2.2}$$

and

$$\frac{\partial}{\partial x}[T \cos \chi] = \rho \frac{\partial^2 v}{\partial t^2} \tag{2.3}$$

respectively where

$$\chi = \tan^{-1}\left(\frac{\frac{\partial y}{\partial x}}{1 + \frac{\partial v}{\partial x}}\right) \quad . \tag{2.4}$$

Equations (2.2) and (2.3) reduce quite simply to the linear equations if $\frac{\partial y}{\partial x} \ll 1$ and $\frac{\partial v}{\partial x} \ll 1$, so that (2.1) becomes

$$T - T_0 \approx ES\frac{\partial y}{\partial x} \tag{2.5}$$

and, from $\chi \approx \sin \chi \approx \frac{\partial y}{\partial x}$ and $\cos \chi \approx 1$, (2.2) becomes

$$T\frac{\partial^2 y}{\partial x^2} = \rho \frac{\partial^2 y}{\partial t^2} \tag{2.6}$$

and (2.3) becomes

$$\rho \frac{\partial^2 v}{\partial t^2} = 0 \quad . \tag{2.7}$$

Carrier solves the nonlinear equations by using a perturbation procedure. Fig. 2.2 shows how the ratio of nonlinear period to linear period varies with $\frac{\Delta T}{T}$, which is essentially (amplitude)^2. Thus one may understand why a string plucked with a fairly large amplitude "twangs" as the amplitude decays with time. Fig. 2.3 shows results for the variation in nonlinear period with the tension at rest position, for three different values of $\frac{T}{ES}$.(amplitude), a graphical representation of why steel strings with a relatively high modulus of elasticity "twang" so much more noticeably than gut strings which have a lower modulus.

Carrier also looks at the three-dimensional problem by allowing deflections in the plane of z normal to the plane of y and shows how the string may vibrate so that each particle follows a quasi-elliptical path. This was shortly followed by a letter (Harrison 1948) in

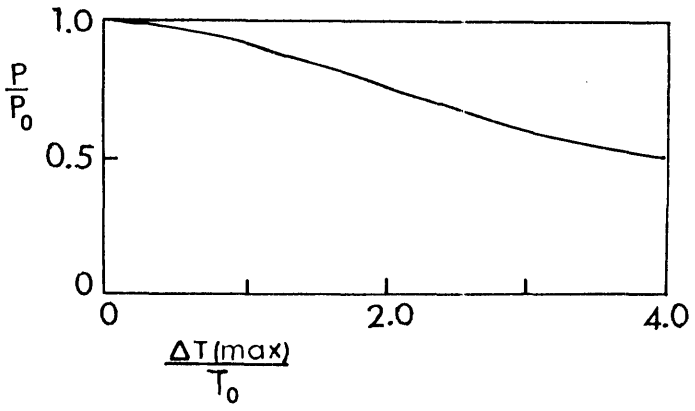

Figure 2.2: Comparison of periods obtained by linear and nonlinear theories (from Carrier 1945). $\frac{P}{P_0} = \frac{\text{nonlinear period}}{\text{linear period}}$; $\frac{\delta T}{T_0} \propto (\text{amplitude})^2$.

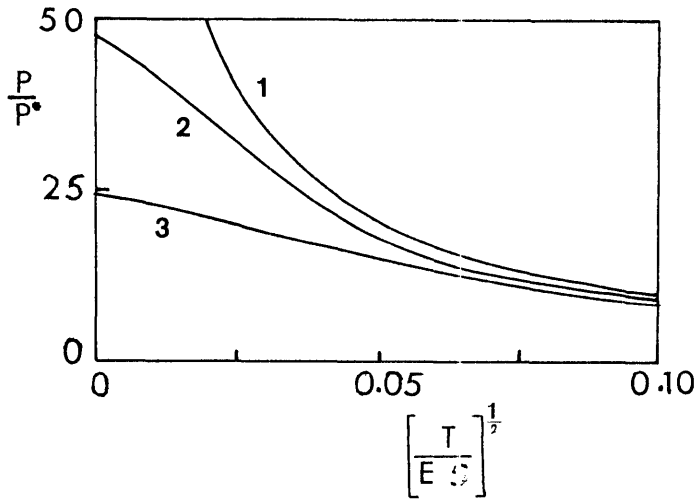

Figure 2.3: Period v.s. initial tension. (1) Vanishing amplitude (linear theory) (2),(3) Increased amplitude.(From Carrier 1945).

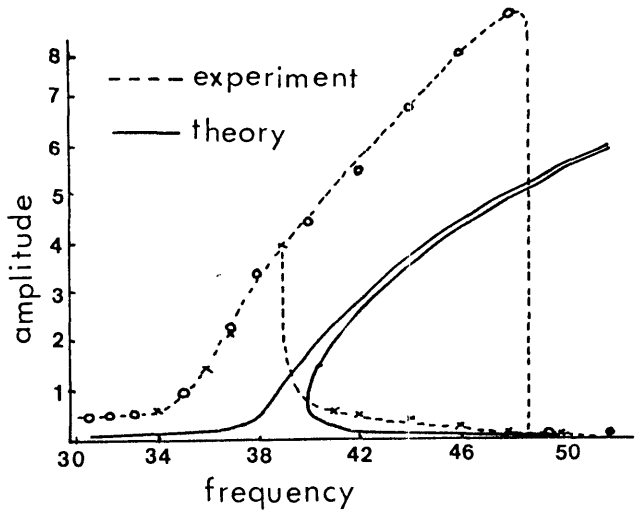

Figure 2.4: Amplitude-frequency characteristics of a string in its fundamental mode (from Lee 1957).

which the author reports on an experiment whereby he observed such circular vibration of a string forced to vibrate near its fundamental frequency. While Harrison offers a qualitative explanation for the phenomenon as an "autoparametric excitment as considered by the Mathieu-Hill theory" he does not attempt any analytical study of it.

It was Lee (1957) who extended Carrier's theory to include forced vibrations near resonant frequencies. Lee introduces an approximation to Carrier's equation for tension (2.1) , by assuming $v = 0$ and $\frac{\partial y}{\partial x}$ is small, although not negligible as assumed by the linear theory, so that the change in tension then becomes

$$T - T_0 = \frac{1}{2} ES \left(\frac{\partial y}{\partial x} \right)^2 . \tag{2.8}$$

This approximation is later justified by Murthy and Ramakrishna (1965) who claim that since Carrier assumed that the string vibrates with an amplitude such that it obeys Hooke's Law and that for most materials departures from Hooke's Law occurs before θ becomes large one may quite easily assume that θ and hence $\frac{\partial y}{\partial x}$ are small compared with unity.

Lee attempts to demonstrate both theoretically and experimentally two effects; a jump phenomenon whereby discontinuities in the amplitude of vibration are observed as the driving frequency is changed, and a hysteresis effect as the frequency for which these jumps occur depends on whether the freqency is being increased or decreased. Fig. 2.4 shows that Lee gets good qualitative results, however, his theoretical calculations were fairly limited and

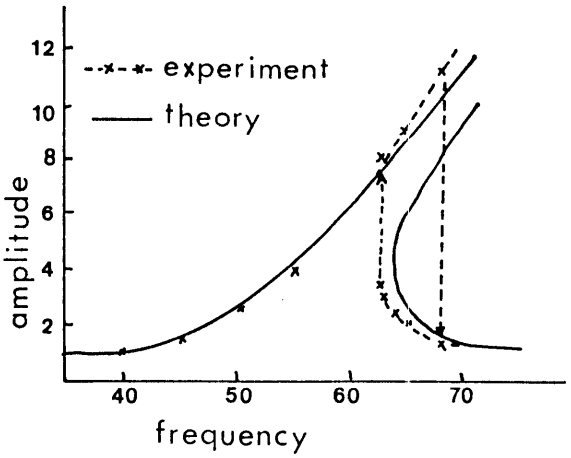

Figure 2.5: Comparison of theoretical and experimental results of the amplitude-frequency characteristics of a string (from Oplinger 1960).

quantitative agreement seems to elude him.

Oplinger (1960) considerably extends Lee's theory so as to cover both amplitude of motion and tension vibration as functions of frequency. In addition he simplifies the equations of motion by assuming that, provided the longitudinal wave speed is very much greater than the transverse wave speed, then the tension will tend to remain uniform along the length of the string and may therefore be written as

$$T \approx T_0 + \frac{ES}{2L} \int_0^L \left(\frac{\partial y}{\partial x}\right)^2 dx \quad . \tag{2.9}$$

This in turn, produces an equation of motion for the string

$$\frac{\partial y^2}{\partial t^2} - c^2 \left[1 + \frac{ES}{2T_0 L} \int_0^L \left(\frac{\partial y}{\partial x}\right)^2 dx\right] \frac{\partial^2 y}{\partial x^2} = 0 \tag{2.10}$$

where $c^2 = \frac{T_0}{m}$.

Oplinger solves this equation by assuming a periodic driving function and separating the variables of $y(x,t)$. This leads to solutions that are elliptic cosine functions. His experimental results show quite good agreement with theory (Fig. 2.5) . It is interesting to note, however, that although he reports on the presence of the out-of-plane vibrations and even mentions that Harrison had previously observed them, Oplinger does not attempt to explain their presence but merely hopes to eliminate them by use of a slot parallel to the motion under observation.

Murthy and Ramakrishna (1965) seek to explain not only the jump phenomena and hysteresis effects investigated by Lee and Oplinger but also the so far neglected out-of-plane vibrations of the forced string. This they do by considering the motion of the string in two perpendicular planes, much the same as Carrier did some twenty years earlier for the free vibrations of a string.

An element of the string is then considered to be deformed into the space element ds, so that

$$ds = (dx^2 + dy^2 + dz^2)^{\frac{1}{2}} \tag{2.11}$$

and the local tension in the string may be written as

$$\begin{aligned} T &= T_0 + ES\frac{ds - dx}{dx} \\ &\simeq T_0 + ES\left\{\frac{1}{2}\left[\left(\frac{\partial y}{\partial x}\right)^2 + \left(\frac{\partial z}{\partial x}\right)^2 - \frac{1}{8}\left(\left(\frac{\partial y}{\partial x}\right)^2 + \left(\frac{\partial z}{\partial x}\right)^2\right)\right]\right\}. \end{aligned} \tag{2.12}$$

Assuming that there is an externally applied force, $f(x)\cos\omega t$ per unit length and using Hamilton's principle of a vanishing first variation of the Lagrangian $L = KE - PE$ together with the clamped end conditions, Murthy and Ramakrishna derive the following equations of motion

$$\frac{\partial^2 y}{\partial t^2} - c_t^2\frac{\partial^2 y}{\partial x^2} - \frac{3}{2}c_l^2\frac{\partial^2 y}{\partial x^2}\left(\frac{\partial y}{\partial x}\right)^2 - \frac{1}{2}c_l^2\frac{\partial}{\partial x}\left(\frac{\partial y}{\partial x}\left(\frac{\partial z}{\partial x}\right)^2\right) = \frac{1}{m}f(x)\cos\omega t \tag{2.13}$$

and

$$\frac{\partial^2 z}{\partial t^2} - c_t^2\frac{\partial^2 z}{\partial x^2} - \frac{3}{2}c_l^2\frac{\partial^2 z}{\partial x^2}\left(\frac{\partial z}{\partial x}\right)^2 - \frac{1}{2}c_l^2\frac{\partial}{\partial x}\left(\left(\frac{\partial y}{\partial x}\right)^2\frac{\partial z}{\partial x}\right) = 0 \tag{2.14}$$

in which c_t and c_l represent the transverse and longitudinal velocities as they are for the linear string. Clearly, if $z = 0$ initially, then it will stay zero but if $z \neq 0$ then the tension will parametrically excite oscillations in the $z-$plane at frequency ω, and so the string will whirl. The particular solutions to the equations obtained by the authors show remarkable agreement with the experimentally obtained response of a forced string as can be seen in Fig. 2.6.

By the time Morse and Ingard (1968) had revised and extended Morse's original text, nonlinear oscillations were regarded as sufficiently important that a whole chapter is devoted to them of which a sizable segment considers large-amplitude string vibrations. They solve, however, for the more general case, when longitudinal motion is not neglected, and so require three coupled nonlinear equations instead of the two deduced by Murthy and Ramakrishna.

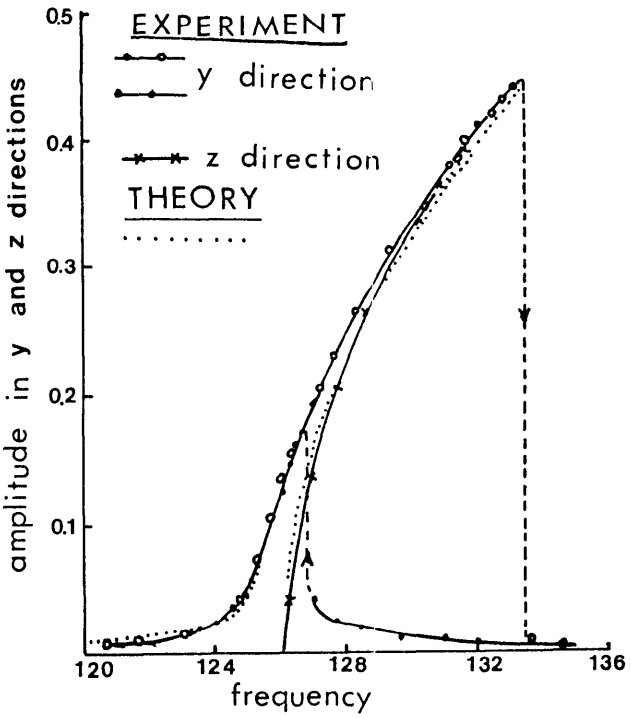

Figure 2.6: Experimentally observed amplitude-frequency response of the string in the y and z planes compared with the theoretical curves (from Murthy and Ramakrishna 1965).

The equations, which quite obviously reduce to the linear equations of motion if second and higher order terms are omitted, are

$$\begin{aligned}
\frac{\partial^2 v}{\partial t^2} - c_l^2 \frac{\partial^2 v}{\partial x^2} &= \frac{1}{2}(c_l^2 - c_t^2)\frac{\partial}{\partial x}\left[\left(\frac{\partial y}{\partial x}\right)^2 + \left(\frac{\partial z}{\partial x}\right)^2 \left(1 - 2\frac{\partial v}{\partial x}\right)\right] \\
\frac{\partial^2 y}{\partial t^2} - c_t^2 \frac{\partial^2 y}{\partial x^2} &= \frac{1}{2}(c_l^2 - c_t^2)\frac{\partial}{\partial x}\left[\frac{\partial y}{\partial x}\left(\left(\frac{\partial y}{\partial x}\right)^2 + \left(\frac{\partial z}{\partial x}\right)^2\right) + 2\frac{\partial y}{\partial x}\frac{\partial v}{\partial x}\left(1 - \frac{\partial v}{\partial x}\right)\right] \quad (2.15) \\
\frac{\partial^2 z}{\partial t^2} - c_t^2 \frac{\partial^2 y}{\partial x^2} &= \frac{1}{2}(c_l^2 - c_t^2)\frac{\partial}{\partial x}\left[\frac{\partial z}{\partial x}\left(\left(\frac{\partial y}{\partial x}\right)^2 + \left(\frac{\partial z}{\partial x}\right)^2\right) + 2\frac{\partial z}{\partial x}\frac{\partial v}{\partial x}\left(1 - \frac{\partial v}{\partial x}\right)\right]
\end{aligned}$$

(where v again represents the longitudinal displacement along the x axis) and show coupling not only between the two transverse modes but also between longitudinal and transverse modes. It is pointed out that this latter coupling may also, in some circumstances, be an important source of indirect coupling between transverse modes.

Following the documenting of nonlinearity for the large-amplitude vibrations of a string in standard texts, there have been a few more papers dealing, in most part, with the nonplanar vibrations or the whirling of the string. In particular Anand(1969) and Gough (1983) both revert to Carrier's original problem of nonlinear free vibrations of the string but use Morse and Ingard's equations of motion to include longitudinal motion.

The nonlinearity of the string is undeniably well established but existing treatments provide little insight into the present problem, namely the coupling between transverse modes of different frequencies within the same plane of vibration. It is with this in mind that we shall spend the next chapter investigating, both theoretically and experimentally, the more general situation in which the supports of the string are not completely rigid.

Chapter 3

Nonlinear generation of missing modes on a vibrating string.

Consider the string shown in Fig. 3.2(a). It is stretched with tension T between two supports, one at $x = 0$ which is rigid and one at $x = L$ which is rigid in the x direction but which has a mechanical admittance (velocity/force) equal to $Y_B(\omega)$ in the y direction at angular frequency ω. Such an arrangement is analogous to that of a string on a piano, harpsichord, or guitar, the compliant support being the bridge that is attached to the soundboard. There are, however, important differences between this idealised situation and a more realistic model of a musical instrument bridge such as shown in Fig. 3.2(b). We shall return to this point later.

If we assume, as is usually true in practice, that the tension is low enough that the velocity of transverse waves on the string is very much less than that of longitudinal waves (Murthy and Ramakrishna 1965) then the tension T can be taken as uniform along the string, and the displacement y, assumed to lie in a single plane as is appropriate for our experiment to be described later, obeys the equation

$$\rho \frac{\partial^2 y}{\partial t^2} = T \frac{\partial^2 y}{\partial x^2} - D \frac{\partial y}{\partial t} \quad , \tag{3.1}$$

where ρ is the mass of the string per unit length, and the coefficient D is a measure of the viscous losses to the surrounding air and internal to the string itself.

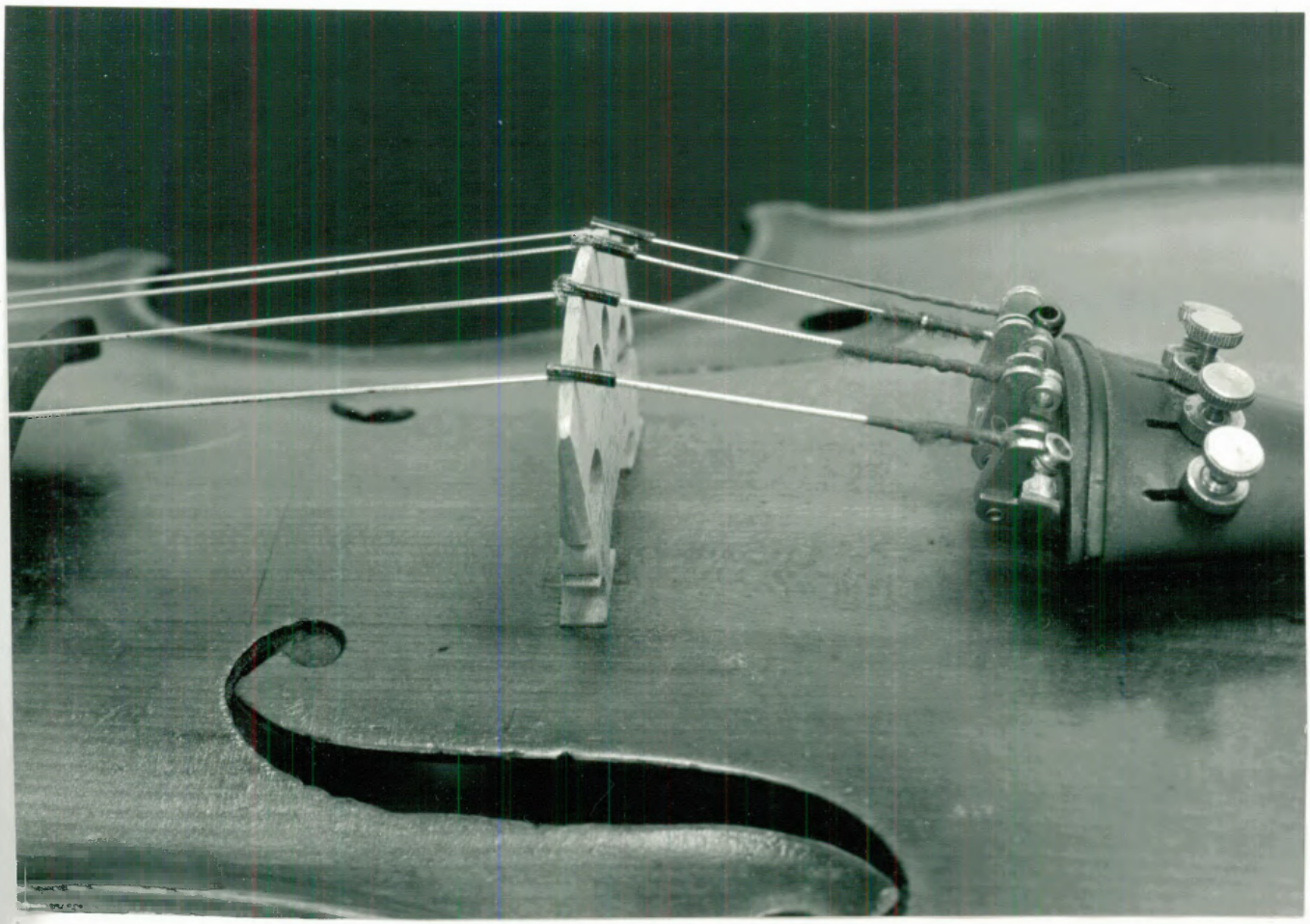

Figure 3.1: The string and bridge arrangement of a violin

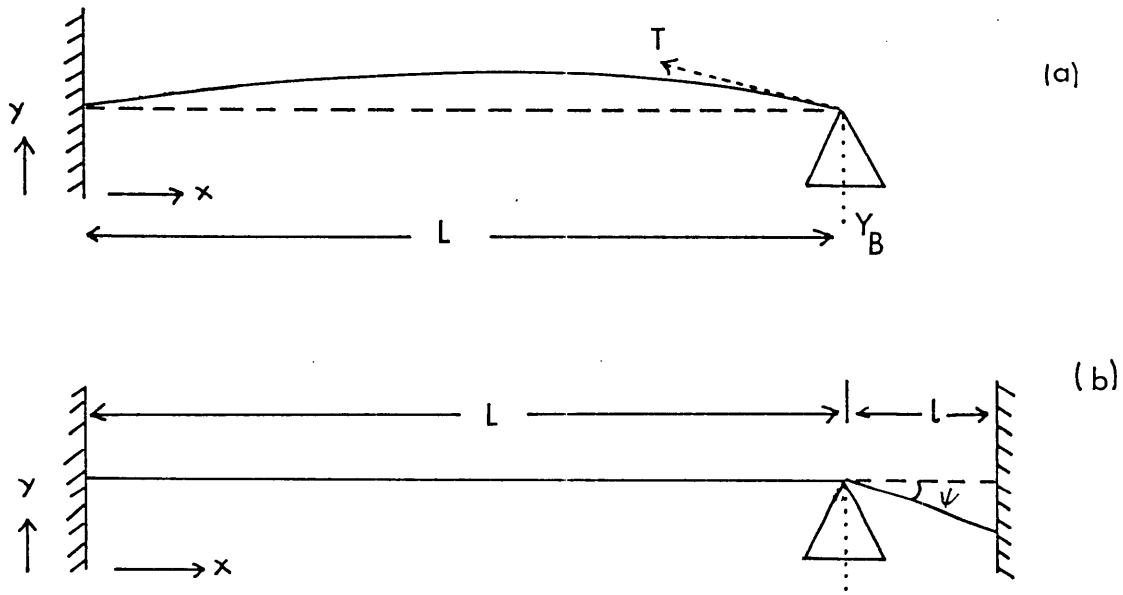

Figure 3.2: The system to be analysed. A flexible string under tension T is atta.:hed to a rigid support at $x = 0$, and its other end is atta ched to a bridge with lateral mechanical admittance Y_B. (a) shows a highly idealised system while (b) is a closer approximation to reality.

3.1 Rigid Supports

The elementary solution for this problem is well known (Morse 1948) when both supports are rigid, so that $Y_B(\omega) = 0$. The damped normal modes have the form

$$y_n(x,t) = a_n \sin\left(\frac{n\pi x}{L}\right) \sin(\omega_n t + \phi_n) \exp\left(\frac{-t}{\tau}\right), \tag{3.2}$$

where

$$\omega_n = \left[\left(\frac{n\pi c}{L}\right)^2 - \left(\frac{1}{\tau_n}\right)^2\right]^{\frac{1}{2}} \approx \frac{n\pi c}{L}$$

$$\tau = \frac{2\rho}{D(\omega)} \text{and} \quad c = \left(\frac{T}{\rho}\right)^{\frac{1}{2}}. \tag{3.3}$$

Finite stiffness of the string raises all angular frequencies ω_n and introduces further inharmonicity (Morse 1948). But since this effect is both small and nearly independent of amplitude, in the interest of algebraic simplicity we ignore it in our discussion. The fundamental nonlinearity, as has been mentioned in the previous chapter, arises because of

the second-order change in the length of the string with vibration amplitude. This length increase is given by

$$\Delta = \int_0^L \left[1 + \left(\frac{\partial y}{\partial x}\right)^2\right]^{\frac{1}{2}} dx - L \tag{3.4}$$

so that the tension becomes

$$T = T_0 + \frac{ES\Delta}{L} \tag{3.5}$$

where E is the Young's modulus of the string material and S is the string's cross-sectional area. Inserting a sum $y = \sum_n y_n$ of the form (3.2), into (3.4) and neglecting terms of fourth or higher order in $\left(\frac{a}{L}\right)$ gives

$$T \approx T_0 + \frac{\pi^2 ES}{8L^2} \sum_n n^2 a_n^2 \left[1 - \cos 2(\omega_n t + \phi_n)\right] \exp \frac{-2t}{\tau_n} \quad . \tag{3.6}$$

The first part of the sum in this expression gives a quasi-static increase in the tension, varying as $\sum_n n^2 a_n^2 \exp\left(\frac{-2t}{\tau_n}\right)$. This causes, from (3.3), a proportional increase in the frequencies of all the modes, the increase dying away with time, and is responsible for the characteristic twang of vigorously plucked strings, particularly if they are of metal rather than gut or nylon, so that the Young's modulus E is high. The remaining terms in the summation contribute oscillatory components of the tension, the frequency 2ω being associated with mode n.

Including (3.6) in the equation of motion (3.1) and multiplying both sides of the resulting equation by the spatial part of the p^{th} mode y_p namely $\sin\frac{p\pi x}{L}$, then integrating over $x = 0$ to $x = L$ removes all terms except those varying like $\sin(p\pi x)$ leaving

$$\frac{d^2 u_p}{dt^2} + \omega_p^2 u_p = \frac{\pi^2 ES}{8\rho L} \sum_n n^2 a_n^2 \left[1 - \cos 2(\omega_n t + \phi_n)\right] \exp\left(\frac{-2t}{\tau_n}\right) u_p - \frac{D_p}{\rho}\frac{du_p}{dt} \tag{3.7}$$

where

$$u_m = a_m \sin(\omega_m t + \phi_m) \quad . \tag{3.8}$$

The differential equation (3.7) for the p^{th} mode has the general form

$$\frac{d^2 u_p}{dt^2} + \omega_p^2 u_p = g(t) \tag{3.9}$$

where the function g contains both damping and forcing terms and depends upon the amplitudes of all the other mode vibrations. This equation is in the standard form for treatment by the method of slowly varying parameters discussed in Chapter 1, for which

each of the modes u, is assumed to have the form as described in (3.8) where a and ϕ are slowly varying functions of t. The further assumption that

$$\frac{du_p}{dt} = a_p(t)\omega_p \cos\left[\omega_p t + \phi_p(t)\right] \tag{3.10}$$

establishes a limitation on the allowed forms of a and ϕ. Finally with (3.8) and (3.10) substituted into (3.9), the resulting equation is multiplied by $\cos\theta$ or $\sin\theta$, where θ is given by

$$\theta_p = \omega_p t + \phi_p \tag{3.11}$$

and averaged over one period $\frac{2\pi}{\omega}$, all terms being neglected except those that change slowly over this time. The resulting equations are

$$\begin{aligned} \langle \dot{a_p} \rangle &= \frac{1}{2\pi\omega_p} \int_0^{2\pi} g(t) \cos\theta_p \, d\theta_p \\ &= \frac{-D}{2\rho} a_p \end{aligned} \tag{3.12}$$

and

$$\begin{aligned} \left\langle \dot{\phi_p} \right\rangle &= \frac{-1}{2\pi\omega_p a_p} \int_0^{2\pi} g(t) \sin\theta_p \, d\theta_p \\ &= \frac{ES\Delta}{L} \left(\frac{p\pi}{L}\right)^2 \frac{1}{2\rho\omega_p} \quad . \end{aligned} \tag{3.13}$$

Thus the change in amplitude of a particular harmonic is proportional to the initial amplitude and contributes a simple damping factor. The frequency however changes like the change in tension. The lack of any dependance of $\langle \dot{a_p} \rangle$ on a_q for $q \neq p$ shows that a string held between two rigid bridges cannot experience the mode conversion we wish to understand. We must therefore turn our attention to the case in which the admittance $Y_B(\omega)$ of the support at $x = L$ is finite.

3.2 Compliant bridge at $x = L$

Consider again Fig. 3.2(a). When the string is in equilibrium the supports are in equilibrium too and this may be taken as the reference position for their displacements. When the string is displaced, however, there will be a component of the tension equal to $T \sin\chi$, where χ is the angle the displaced string makes with its equilibrium position, acting on the support. In the linear approximation χ is assumed to be small so that $\sin\chi = \tan\chi$ which is equal to

the slope of the string at $x = L$. If the support at $x = L$ has finite mechanical admittance $Y_B(\omega)$ then the termination condition at this bridge is just

$$\left.\frac{\partial y}{\partial t}\right|_{x=L} = -Y_B T_0 \left.\frac{\partial y}{\partial x}\right|_{x=L} \quad . \tag{3.14}$$

The termination condition at $x = 0$, a rigid support, remains

$$y(0,t) = 0 \quad . \tag{3.15}$$

It would be possible to apply this condition without restriction to the lossy string described by (3.1),but it helps the clarity of the argument and is also adequate for our practical purposes to make some simplifying assumptions. The first of these is that the bridge admittance $Y_B(\omega)$ is always small compared with the characteristic admittance $\frac{1}{\rho c}$ of the string so that the bridge is nearly a node for the string motion. The second is that the energy losses in the system can be partitioned between those at the bridge, giving decay time constants τ_n' , and those associated with viscous or internal losses along the string, giving decay constants τ_n'' , so that the combined decay constant τ_n is given by

$$\frac{1}{\tau_n} = \frac{1}{\tau_n'} + \frac{1}{\tau_n''} \tag{3.16}$$

where it is now τ_n'',rather than τ_n that is related to $D(\omega)$ by (3.3). The third is to assume that the bridge itself behaves as a simple linear system so that $Y_B(\omega)$ can be written as an amplitude-independent complex function of ω when the time-variation of the normal modes (3.2) is written as $\exp(j\omega t)$.

With these assumptions in mind, we follow the procedure outlined by Morse(1948) to derive an expression for the characteristic frequency of the n^{th} mode, remembering that our derivations are an adaption of Morse's as we have only one nonrigid bridge. We assume a characteristic funtion of the form

$$\psi_n(x,\omega_n) = \sin\left(\frac{\omega_n x}{c}\right) \tag{3.17}$$

so that

$$y_n = \sin\left(\frac{\omega_n x}{c}\right)\exp(j\omega t) \tag{3.18}$$

which together with (3.14) leads to

$$\omega_n \approx \frac{n\pi c}{L}\left[1 - T_0\frac{Im(Y_B)}{\omega L}\right] \tag{3.19}$$

and

$$(\tau_n'')^{-1} = \frac{T_0 Re(Y_B)}{L} \tag{3.20}$$

where $Re(Y_B)$ and $Im(Y_B)$ are, respectively, the real and imaginary parts of the bridge admittanceY_B.

Equation (3.19) may quite easily be written in the form

$$\omega_n = \frac{n\pi c}{L + \delta_n} \tag{3.21}$$

where

$$\delta_n \approx T_0 \frac{Im(Y_B)}{\omega} \quad . \tag{3.22}$$

Thus the string behaves, for each mode, very much like a normal lossy string supported rigidly at $x = 0$ and $x = L + \delta_n$. The eigenfunctions, for the linear approximation, will still have the form (3.2) but with (3.19) and (3.20) inserted and with L replaced by $L + \delta_n$.

3.3 Nonlinear forcing term

For the more general nonlinear problem to which we now turn, the force on the compliant bridge is, to sufficient accuracy from (3.2) and (3.6)

$$F = -T \frac{\partial y}{\partial x}\Big|_{x=L} \approx \left(T_0 + \sum_n T_n\right) \sum_m A_m \sin\theta_m - \frac{1}{2} \sum_n \sum_m T_n A_m \sin(\theta_m \pm 2\theta_n) \tag{3.23}$$

where

$$\begin{aligned} T_n &\approx \left(\frac{\pi^2 ES}{8L^2}\right) n^2 a_n^2 \exp(\frac{-2t}{\tau_n}) \\ A_n &\approx (-1)^{n+1} \left(\frac{\pi}{l}\right) n a_n \exp(\frac{-t}{\tau_n}) \end{aligned} \tag{3.24}$$

and

$$\theta_n \approx \omega_n t + \phi_n \tag{3.25}$$

the approximations arising from neglecting δ_n in comparison with L in appropriate places.

The force F acts upon the compliant bridge and its attached string, which are mechanically in series since they have the same displacement velocity. To the approximation to which we are working, the problem is thus equivalent to that of a rigidly supported string of length $L + \delta_n$, acted upon by the force F at the point $x = L$, which is a distance δ_n from

one end. The resistive part $Re(Y_B)$ of the bridge admittance may also be localized at this point.

The equation of motion for the string is now formally, comparing with (3.1),

$$\rho\frac{\partial^2 y}{\partial t^2} = T_0\frac{\partial^2 y}{\partial x^2} - D\frac{\partial y}{\partial t} - R'\frac{\partial y}{\partial t}\delta(x-L) + F(t)\delta(x-L) \tag{3.26}$$

where $y = 0$ at $x = 0$ and $x = L + \delta_p$ for the p^{th} mode, the form of which is given by (3.2) with L replaced by $L + \delta_p$ and with δ_p given by (3.22). The form of R' is clearly related to τ'' by (3.20) but need not concern us for the moment.

Multiplying (3.26) by the spatial part of y_p , namely $\sin\left(\frac{p\pi x}{L+\delta_p}\right)$, and integrating over $x = 0$ to $L + \delta_p$ gives

$$\rho\frac{\partial^2 u_p}{\partial t^2} = -T_0\left(\frac{p\pi}{L+\delta_n}\right)^2 u_p - R\frac{\partial u_p}{\partial t} + \frac{2}{L}F(t)\sin\frac{p\pi L}{L+\delta_p} \tag{3.27}$$

where R is related to D and R', and the p^{th} normal mode is now represented by

$$u_p = a\sin(\omega_p t + \phi_p) \tag{3.28}$$

when $F = 0$. This serves, if we wish, to relate R to τ_p . Using (3.3), assuming $\delta_p \ll \frac{L}{p}$, and then using (3.22), we can rewrite (3.27) as

$$\frac{\partial^2 u_p}{\partial t^2} + \omega_p u_p = \frac{-2}{\tau_p}\frac{\partial u_p}{\partial t} - (-1)^p\frac{2p\pi}{\rho\omega_p L^2}T_0 Im(Y_B)F(t) \tag{3.29}$$

There is an equation of this form for each of the modes p. In cases of practical interest, the damping is small so that $\tau_p \ll \frac{1}{\omega_p}$ and the resonances are so narrow that only those terms in $F(t)$ with frequencies very close to ω_p need to be considered. We note, incidently, that the forcing term involving $F(t)$ is proportional to the bridge admittance Y_B , and so vanishes for a string supported on rigid bridges, in agreement with our earlier discussion.

3.4 First-order solution

The differential equation (3.26) for the p^{th} mode has the general form (3.9) and may be solved using the method of slowly varying parameters as described earlier for the case of rigid supports. The resulting equations are

$$\langle\dot{a}\rangle = \sum_n\sum_m \beta_p a_m a_n^2 \sin\left[(\omega_m \pm 2\omega_n \pm \omega_p)t + (\phi_m \pm 2\phi_n \pm \phi_p)\right] - \frac{a_p}{\tau_p} \tag{3.30}$$

and

$$\left\langle \dot{\phi}_p \right\rangle = \sum_n \sum_m \frac{\pm \beta_p a_m a_n^2}{a_p} \cos\left[(\omega_m \pm 2\omega_n \pm \omega_p) + (\phi_m \pm 2\phi_n \pm \phi_p)\right] \tag{3.31}$$

where only the terms $m \pm 2n \pm p = 0$ are retained. The mode coupling coefficients β_p are given by

$$\beta_p = \frac{\pi^4 T_0 E S}{32 \rho L^5 \omega_p^2} Im(Y_B) \quad . \tag{3.32}$$

It is also important to note that in the expressions (3.30) and (3.31) the $\pm$ before ω_p is independent of that before $2\omega_n$ but tied to the leading $\pm$ in (3.31). The signs of the ϕ_j follow those of their related ω_j. Hence we see that modes m and n will couple to generate mode p only if $m \pm 2n = \pm p$.

A solution to the general problem thus requires consideration of the pairs of coupled equations (3.30) and(3.31) for all modes of the string. For our present problem, however, a much simpler procedure suffices. Suppose the string is excited so that only two modes n and m have appreciable amplitude, and a third mode of interest, p, has zero initial amplitude. We further suppose that modes n and m are either not coupled, in the sense that $m \pm 2n \neq |m|$, $3n \neq m$, and similarly with m and n interchanged, or that any such coupling is small enough to be neglected. Then the forcing term F will be zero at mode frequencies ω_m and ω_n, as can be seen by (3.23), except for some small self-interaction which simply lead to frequency shifts as in (3.13), and each of these modes will decay exponentially as shown by

$$a_n = a_n^0 \exp\left(\frac{-t}{\tau_n}\right) \tag{3.33}$$

$$a_m = a_m^0 \exp\left(\frac{-t}{\tau_m}\right) \quad . \tag{3.34}$$

If n and m are chosen so that one or more of the combinations $|m \pm 2n|$, $|n \pm 2m|$ (including $3n$ or $3m$) is equal to p, however, then the forcing term F for mode p will not vanish.

In the simple case in which ω_m and ω_n are harmonically related, the frequencies of these driving terms near ω_p will be the same, although not nesessarily exactly equal to ω_p unless it too is part of the same harmonic relationship. Provided the dicrepancy between ω_p and the driving frequency is not too large, the phase of mode p (which is initially undetermined) can adopt a value such that the actual oscillation frequency ω_p' ,given by (3.8) as

$$\omega_p' = \omega_p + \langle \dot{\phi}_p \rangle \tag{3.35}$$

is equal to the driving frequency. This is simply the phenomenon of off-resonance driving as expressed in this formalism. Once the initial phase ϕ has been determined in this way, $\langle\dot{\phi}_p\rangle$ remains nearly constant, only tracking the quasi-static tension change, and the value of $\langle\dot{a}\rangle$ can be determined. There is an inverse relationship between the magnitude of these two quantities, given explicitly by (3.30) and (3.31), as is always the case for systems slightly away from resonance.

The general problem requires numerical methods at this stage unless the relevant frequencies ω_m and ω_n are harmonically related, for the general solution will involve beats and similar fluctuation phenomena. Suppose, however, that we neglect all driving modes except m and n driving mode p through the coefficient β_p , and let

$$\triangle\,\omega_p = \langle\dot{\phi}_p\rangle = \omega_p' - \omega_p \tag{3.36}$$

Then from (3.31), in abbreviated notation,

$$\cos[\qquad\ ] = \pm\frac{\triangle\omega_p a_p}{\beta_p a_m a_n^2} \tag{3.37}$$

and this can be substituted back into (3.30) to give

$$\langle\dot{a_p}\rangle = \beta_p a_m a_n^2\left[1 - \left(\frac{\triangle\omega_p a_p}{\beta_p a_p a_n^2}\right)^2\right]^{\frac{1}{2}} - \frac{a_p}{\tau_p}\quad . \tag{3.38}$$

It is clear from the general form of (3.38) that, if a_m and a_n are both initially proportional to some pluck amplitude A while a_p is zero, then a_p will rise at a rate proportional to A^3, go through a maximum as a_m and a_n decay, and then decay itself with a time constant tending towards τ_p . It is also clear that the excitation of mode p will be most efficient when all the modes are nearly harmonically related, so that $\triangle\omega_p$ is small, and when the decay times τ are long.

Another conclusion that follows from the general form of (3.38) is that not all modes can be driven by this mechanism but only those for which $p = |2n \pm m|$. In particular if the modes are essentially harmonic and the string is plucked near its centre so that no even modes are excited, then the mechanism cannot provide subsequent excitation of any of these even modes.

3.5 Theory for a realistic bridge

The idealized bridge shown in Fig. 3.2(a) and considered in our theory above differs significantly from the more realistic bridge shown in Fig. 3.2(b). For the realistic bridge structure, it is an adequate approximation for our present purpose to assume that the bridge itself is quite compliant in a direction parallel to the string, with the necessary longitudinal rigidity being provided by the short angled length of string between it and the hitch-pin. We can then assume that the tension T of the string is the same throughout its whole length.

The analysis of the previous section still applies to this structure, with the admittance Y_B being interpreted as applying to the transverse behaviour of the bridge and string tail together. However, as we shall see in a moment, there is also a further nonlinearity of second order rather than third order which can dominate the behaviour in certain cases.

Suppose that the bridge is in equilibrium under tension T_0 and that this tension is increased to T by the mechanism leading to Eq.(3.14). Then, because of the inclination of the tail of the string, this increase leads to an additional force F on the bridge structure of magnitude

$$F(t) = (T - T_0) \sin \psi \quad . \tag{3.39}$$

If the string carries modes m and n, then, from (3.6), $F(t)$ has components of frequencies $2\omega_m$ and $2\omega_n$ with amplitudes proportional to a_m^2 and a_n^2, respectively. There is no frequency mixing below fourth-order terms.

The effect of this force can be treated in exactly the same way as before, and the governing equation is formally identical with (3.26) or (3.29). The solution is given by equations similar to (3.30) and (3.31) or, quite generally since there is only one driving term for each mode, by an equation like (3.38). The only difference is the replacement

$$\beta_p a_m a_n^2 \rightarrow \beta_{np} a_n^2 \sin \psi \tag{3.40}$$

where

$$\beta_{np} = pn^2 \frac{\pi^3 E S T_0}{\rho 8 L^4 \omega_p^2} Im(Y_B) \quad . \tag{3.41}$$

In summary we note that this nonlinearity can drive only even modes, that it behaves as the square rather than the cube of the initial excitation amplitude, and that its coupling magnitude is proportional to $\sin \psi$, where ψ is the bending angle of the string as it passes over the bridge.

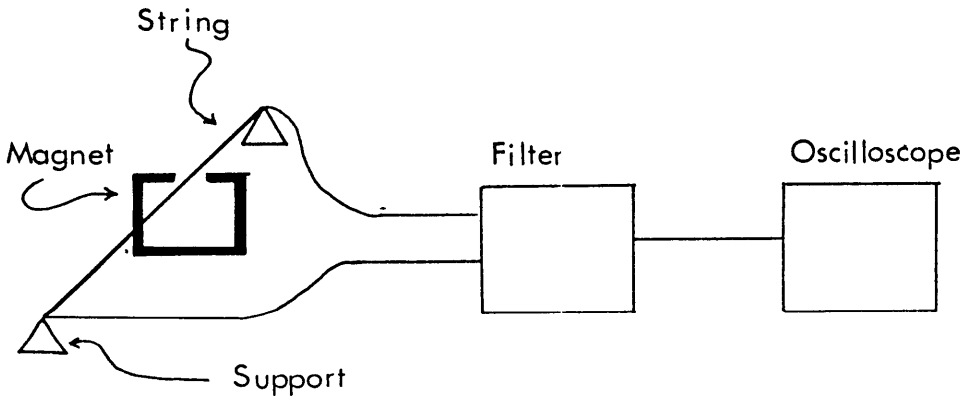

Figure 3.3: A tensioned nichrome wire passing over two bridges 67cm apart and placed in the field of a permanent horseshoe magnet. The *emf* produced by the motion of the string was fed via a filter to a storage oscilloscope.

3.6 Experiment

The experimental arrangement consisted of a tensioned nichrome wire, 0.3 mm in diameter, passing over two rigid bridges about 67 cm apart. The fundamental frequency was about $200Hz$. A horseshoe permanent magnet produced a strong magnetic field normal to the wire over a short part of its length, and the emf produced by motion gave a signal propotional to the velocity of the string in the field region, and hence to appropriately weighted amplitudes of the string vibration modes. The modes were isolated by feeding the signal through a digital filter (Bruel and Kjaer type 1623) with a bandwidth of 12% or 24%, thus giving an adequately short rise time, and were displayed on a storage oscilloscope, using the arrangement shown in Fig.3.3. The relative response of the system to different modes was calibrated as will be described later.

The first check of theory for rigid bridges was performed by plucking the string to a displacement of about 3 mm at one- third of its length, giving large amplitudes to modes 1 and 2 and a carefully defined near-zero amplitude to mode 3. No subsequent increase in the amplitude of mode 3 was observed, in agreement with theoretical prediction. A similar confirmatory null result was found for mode 2 when the string was plucked at its center.

A compliant bridge was constructed by looping a thin, cotton wrapped elastic cord over

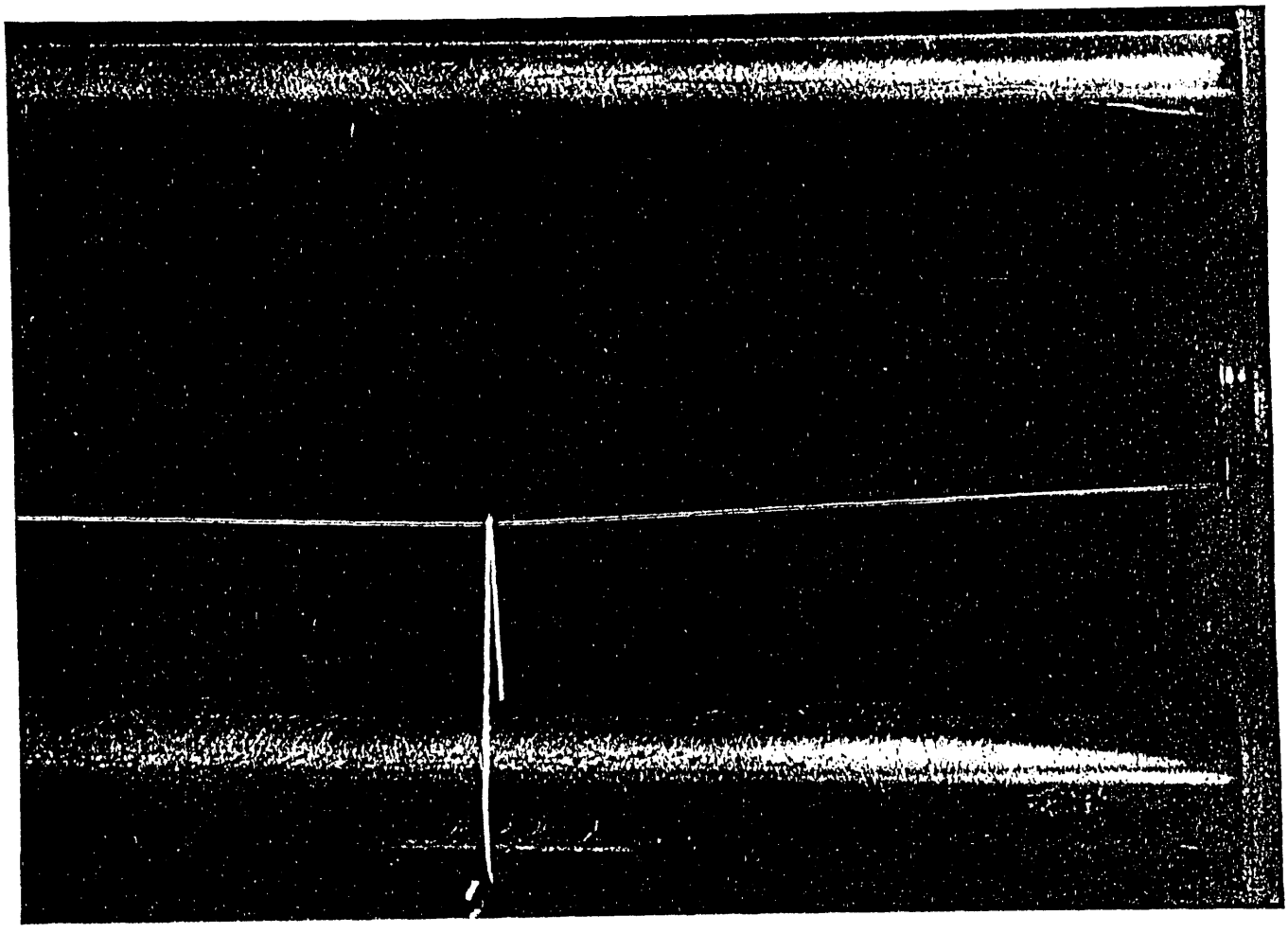

Figure 3.4: The compliant bridge consisting of a thin cotton wrapped elastic cord over the wire securing it to a lower support.

the wire and securing it to a lower support as shown in Fig. 3.4. This arrangement gave a bridge that was not only nearly ideally compliant (ie having a admittance that consisted only of a compliance and a small series resistance), but also very substantially anisotropic. Thus we effectively decouple the two polarizations of wire vibrations and eliminate one source of experimental difficulty namely the whirling of the string as described by Murthy and Ramakrishna (1965). A small pad of rubber damped the short end of the string and minimized undesired high-frequency vibrations without adding a significant resistance to the bridge admittance. The string length L was about 55 cm, the tail length l about 12 cm, and the angle ψ about 3^o .

With this arrangement and using a mechanical plucking device , several series of plucks were recorded on magnetic tape for later analysis. In one series the string was plucked close to its midpoint in a position found to give nearly zero excitation of the second mode, while in the other series a plucking point near one third of the string length was used so as to minimize the initial amplitude of the third mode. In each case a range of pluck amplitudes up to about 3 mm was used.

When the records were replayed for analysis, the modes initially excited were found to decay more or less exponentially with time, while the unexcited modes grew from near zero to a maximum in a time of the order 0.1s and then decayed slowly to zero. A typical trace is shown in Fig. 3.5. To analyze these results, the peak amplitude reached by the missing mode and the time taken to reach this peak were both plotted as functions of the initial fundamental mode amplitude a_1^0 , also derived from the recording. These measurements are shown in Fig. 3.6 for the second mode and in Fig. 3.7 for the third mode.

Comparison with theory must await the discussion of the following section, but we see immediately that the peak amplitude of the "missing" mode, though substantially less than the initial amplitude of the fundamental, is of quite significant magnitude. The amplitude of this peak does not behave in an entirely simple manner in its dependence upon the amplitude a_1^0 of the fundamental in either case, though clearly the maximum values of both a_2 and a_3 increase with increasing a_1^0 . The time delay to the peak amplitude decreases significantly with increasing a_1^0 in both cases, the measured range of variation being as much as a factor of 3 over the amplitude range studied.

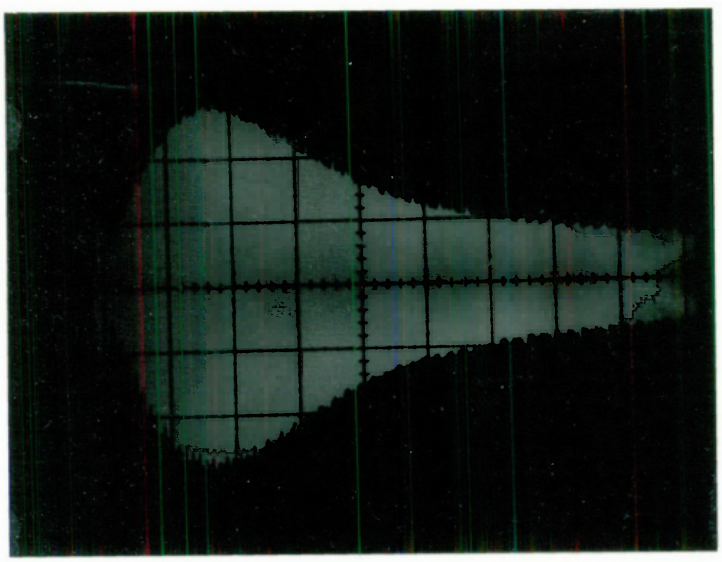

Figure 3.5: Oscilloscope record of the growth and decay of the third vibration mode of the string when it is plucked at a node for that mode. The major graticule divisions are 0.05s apart.

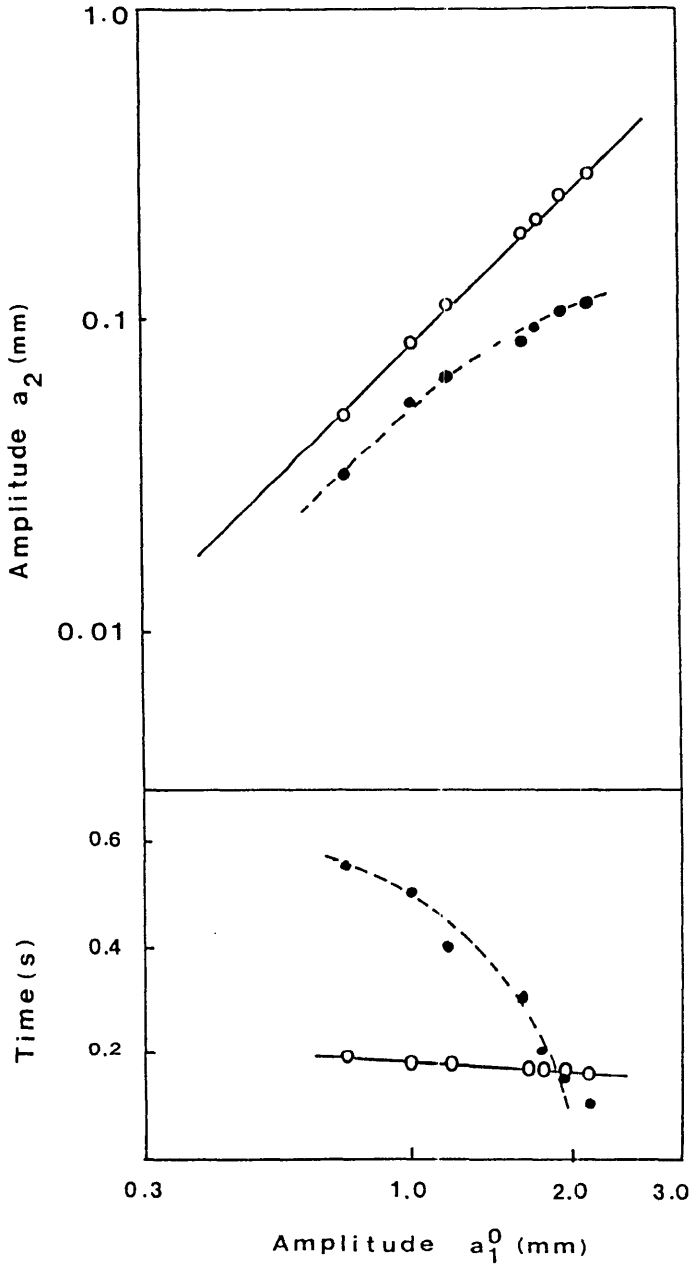

Figure 3.6: Measured values (filled circles, broken curve) and calculated values (open circles, full curve) of the maximum amplitude a_2 achieved by the second mode, and the time to reach this amplitude, as functions of initial amplitude a_1^0 of the first mode.

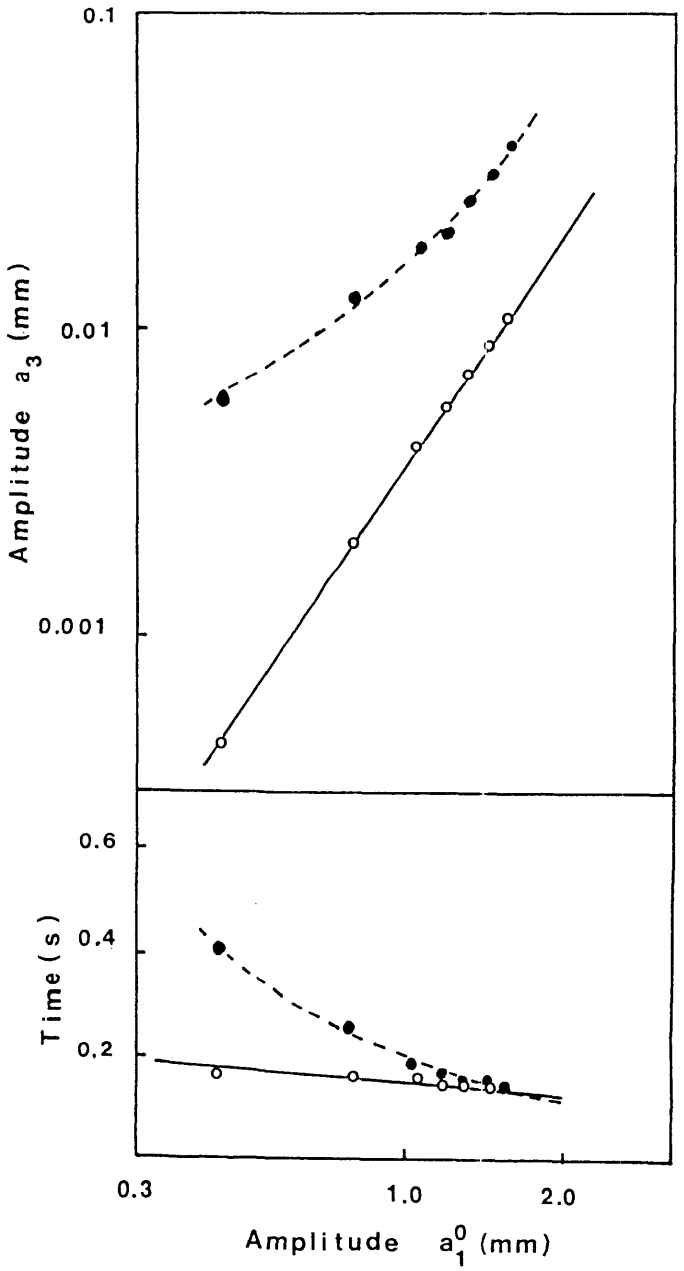

Figure 3.7: Measured values (filled circles broken curve) and calculated values (open circles, full curve) of the maximum amplitude a_3 achieved by the third mode, and of the time to reach this amplitude, as functions of the initial amplitude a_1^0 of the first mode.

3.7 Calibration of amplitude

As has already been mentioned, the motion of the string was measured by placing a horse-shoe magnet over a short part of its length and observing the *emf* induced. Calibration of the system involved vibrating the string electrically, by passing a current of known frequency through it. A travelling microscope was placed so as to observe the string at an antinode of its vibration and the amplitude was measured in millimeters. The current was then switched off and the string was allowed to decay freely with the *emf* subsequently produced being displayed on the oscilloscope screen. It must be noted here that the magnetic field, situated at $\frac{1}{4}$ the length of the string for the purpose of this calibration, produces an emf proportional to the velocity of the motion and this needs to be taken into account when considering the calibration of modes of different frequency.

3.8 Damping

The measurement of the decay of the string for various modes was done using a similar arrangement to that used in the calibration. The string was vibrated at one particular frequency by passing a current through it, the current was then switched off and the decay of the mode was measured. It is important to note here that the current through the string had quite a pronounced effect on its temperature and so, to avoid any change to its characteristics, the string was cooled during the course of the measurements by a fan.

The results obtained introduce a further nonlinearity into the problem which has so far been neglected. Consider the damping term $\frac{-a_p}{\tau_p}$ in (3.30) and (3.38) which accounts for the free decay of mode p. This linear approximation may indeed be adequate in some practical situations, but measurements of the free decay of modes excited singly in our experiment as described above, showed that the time constant τ_p depended significantly on the mode amplitude a_p, with τ_p decreasing considerably for large a_p. Such an effect is indeed expected for the viscous drag exerted on the string by the surrounding air, since the Reynolds number for our vibrating string lay typically in the range 10 to 100, which is just the range over which the drag for steady flow past a cylinder changes from linear to quadratic (Tritton 1977). In our case, however, much of the damping is caused by the bridge structure, for which quite different considerations apply. Nevertheless, the form of equation suggested by

the air-damping analogy, namely

$$\tau_p^{-1} = \alpha_p + \gamma_p a_p \tag{3.42}$$

was found to fit the data quite adequately, with α_p and γ_p as experimentally determined constants (Fig. 3.8).

Clearly, with several modes present on the string simultaneously, as in the experimental plucked situation, we expect interaction terms in the damping. This was confirmed by examining the decay of a particular mode when the string was plucked rather than excited only in that mode. The experimental results may therefore be approximated by the obvious generalization

$$\tau_p^{-1} \approx a_p + \gamma_p a_p + \sum_{n \neq p} \gamma_{np} a_n, \tag{3.43}$$

where only one or two of the more important terms need be included in the summation. Experimental values for the relevant α and γ parameters in $(s)^{-1}$ and $(s\ mm)^{-1}$ respectively are given in the following table for our experimental system.

Mode 1	*Mode 2*	*Mode 3*
$\alpha_1 = 0.4$	$\alpha_2 = 0.7$	$\alpha_3 = 0.08$
$\gamma_1 = 0.6$	$\gamma_2 = 2.5$	$\gamma_3 = 9.2$
$\gamma_{21} = 2.5$		
$\gamma_{31} = 6$	$\gamma_{32} = 12$	

3.9 Admittance of the compliant bridge.

In the experimental arrangement, the bridge consists effectively of the elastic cord together with the oblique end of the string. The static compliance of this combined bridge was found by careful measurement of geometry, followed by a measurement of the amount by which the string deflection at the bridge changed when the string tension was lowered or raised. The behaviour was linear within the accuracy of measurement, and the resulting numerical value was

$$\lim_{\omega \to 0} \omega^{-1} Im(Y_B) \approx 0.6 mm N^{-1}. \tag{3.44}$$

If the real part of Y_B is small, as we shall see in a moment that it is, then this implies from (3.22) a δ value of about 2 cm which does not change very much with frequency. This was checked by noting the change in frequency when the compliant bridge was replaced by a

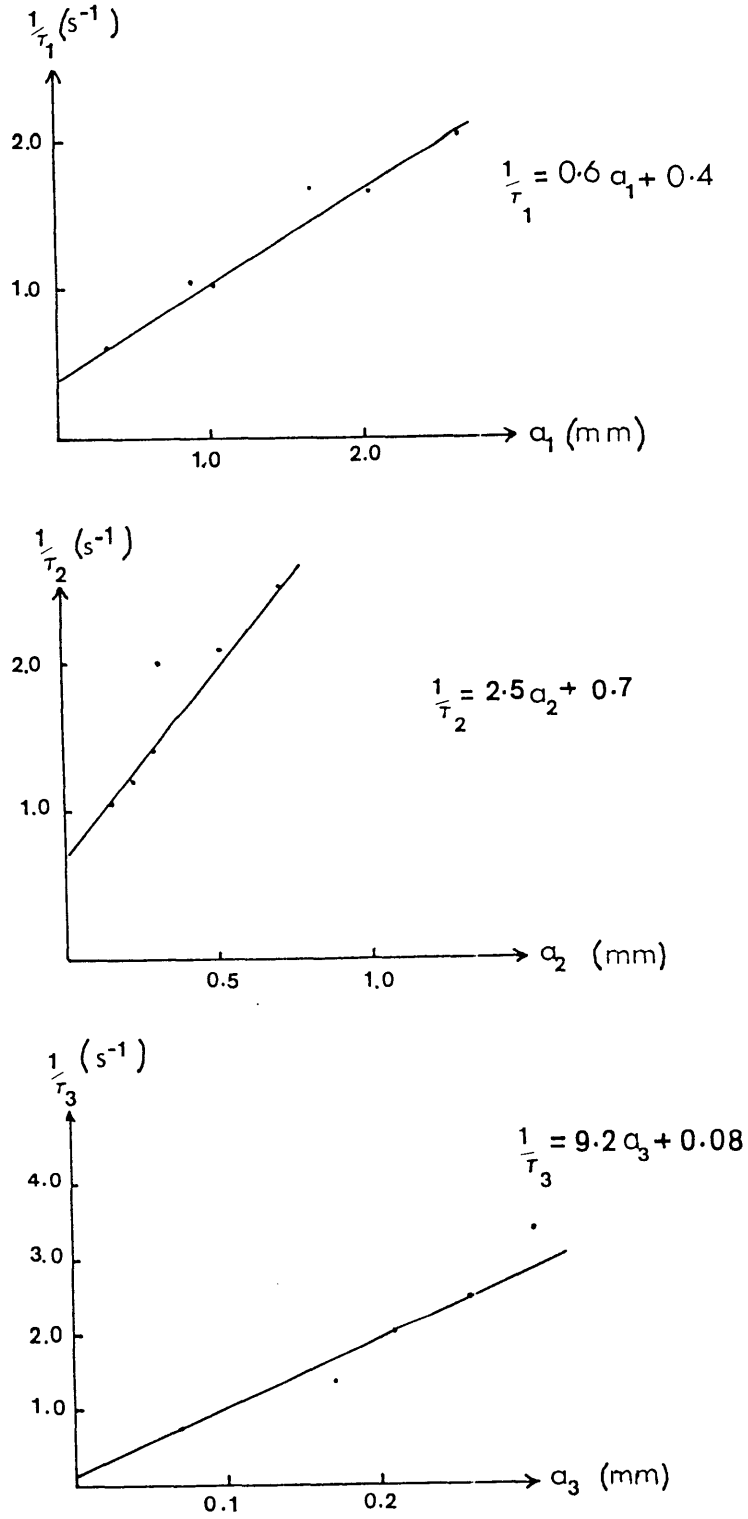

Figure 3.8: Measured values of the decay time for modes 1,2 and 3 plotted inversely against their relevant mode amplitudes.

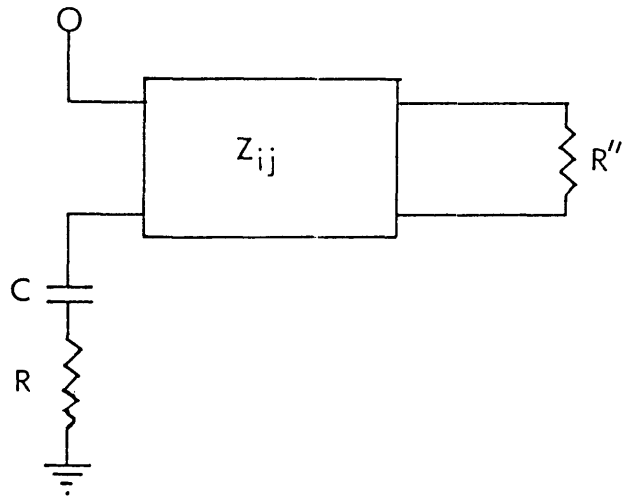

Figure 3.9: Electrical analog cicuit for the mechanical properties of the bridge used in our experimental arrangement. R and C represent the behaviour of the elastic cord, Z_{ij} is the impedance of the tail of the string, and R'' the large resistance with which it terminates. The input admittance of this network is Y_B.

rigid bridge without disturbing either geometry or string tension, and the agreement with calculation was found to be good. The frequencies of the first three modes are harmonically related to a good approximation.

Experiment showed that the insertion of a small rubber pad at the remote end of the string tail made little difference to observed decay times, while the decay time for the string with its compliant bridge is about half that for the same string supported between two rigid bridges. Since the end correction is not very sensitive to the exact value of τ', it is adequate to assume $\tau' = \tau'' = 2\tau_n$ for all n. The bridge may be considered as consisting of a piece of wire cord in series with the end of the nichrome string. Thus its impedance may be written as

$$Z_B = R + \frac{1}{C\omega j} - jZ_0 \cot\left(\frac{\omega l'}{c}\right) \tag{3.45}$$

where C is the bridge's compliance and Z_0 is the characteristic impedance of the string. This equation together with equations (3.19) and (3.20) and the measured τ values and compliances for the complete bridge structure allows for two possible values, respectively of order 10^{-2} and 10^{2} $Nm^{-1}s$, for the effective resistance R in series with the bridge compliance. The smaller value is supported by the relatively large value of δ referred to above. Furthermore an independent measurement of the mechanical admittance of a similar

piece of the same elastic cord using a Bruel and Kjaer type 8001 impedance head to measure its admittance on a Hewlett Packard Spectrum Analyser type 3582A gave an effective series resistance of a few times $10^{-3} Nm^{-1}s$ at 100 Hz, confirming the lower resistance value. The resistance was also found to increase with increasing vibration amplitude, an effect which is directly associated with the change of the τ values with increasing amplitude as discussed previously.

To calculate approximately the frequency variation of the bridge admittance Y_B, an anolog model of the form shown in Fig. 3.9 was used. The 2-port network Z_{ij} represents the tail of the string, the large resistance R'' the effect of the rubber pad at the rigid bridge, and the combination RC the behaviour of the elastic cord. Now R'' is very large compared with the characteristic impedance ρc of the string, as is shown by the negligible effect of R'' on the modes in which we are interested. We can therefore set $R'' = \infty$ to adequate accuracy and replace Z_{ij} by its input impedence

$$Z_{11} = -j\rho c \cot\left(\frac{\omega l'}{c}\right) \tag{3.46}$$

where l' is the length of the string tail. The known low-frequency limit of $Im(Y_B)$ given by (3.44) and the known value of τ_n from (3.42) to give $Re(Y_B)$ then allow all the quantities in the model of Fig. 3.9 to be calculated.

3.10 Numerical solutions

For the purpose of our numerical solutions, the form of (3.43) was simply inserted into (3.19) and (3.20), using the analog circuit of Fig. 3.9 to determine the ω_n and hence $\Delta\omega_p$ at each instant, and then into (3.38) or (3.40) for numerical integration to plot the behaviour of the missing mode amplitude a_p.

In Figs. 3.10 and 3.11 we show the calculated behaviour of the second and third mode amplitudes, when the string is plucked so as to make their respective initial values zero, for the particular string and bridge configuration used in our experiments. Clearly the general predictions of the theory are qualitatively similar to the experimental behaviour shown in Fig. 3.5.

For quantitative assessment of the theory, its predictions of maximum amplitude and time to reach that amplitude are shown by open circles plotted alongside the experimental data (filled circles) in Figs. 3.6 and 3.7. The absolute values of the predicted amplitudes

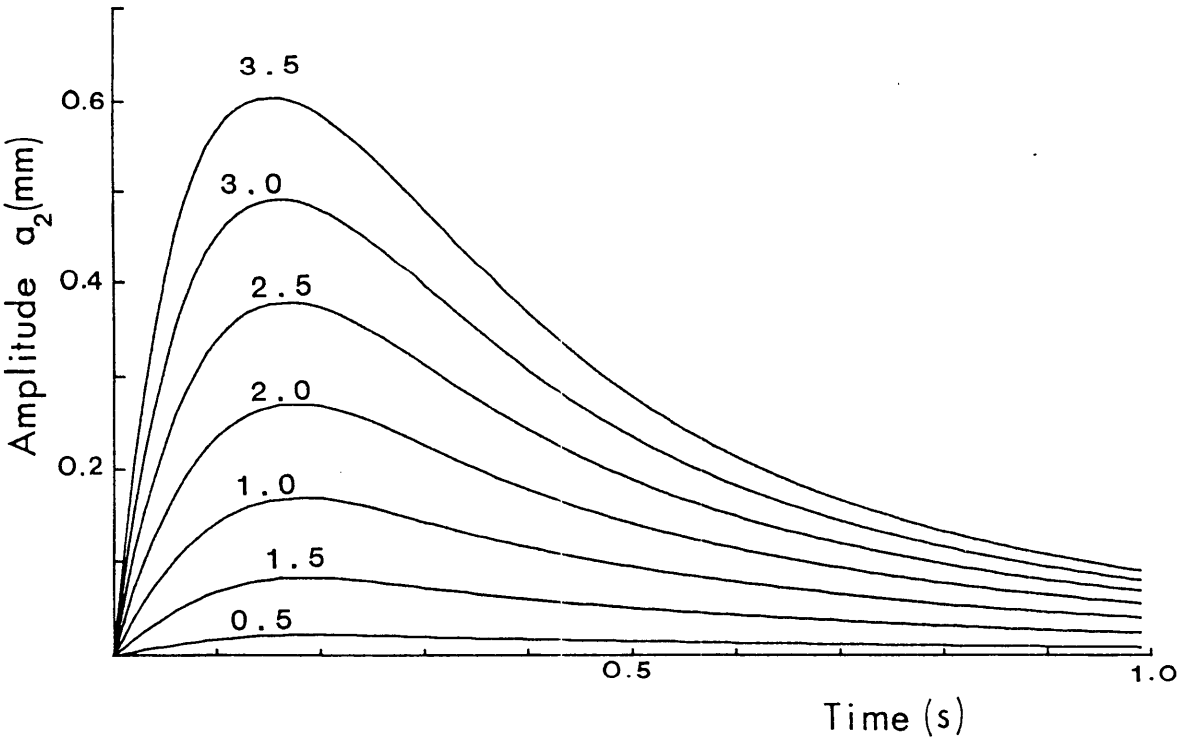

Figure 3.10: Calculated growth and decay of the second mode of the string, plucked at a node for that mode, for first mode amplitudes ranging from 0.5 to 3.5mm (shown as a parameter).

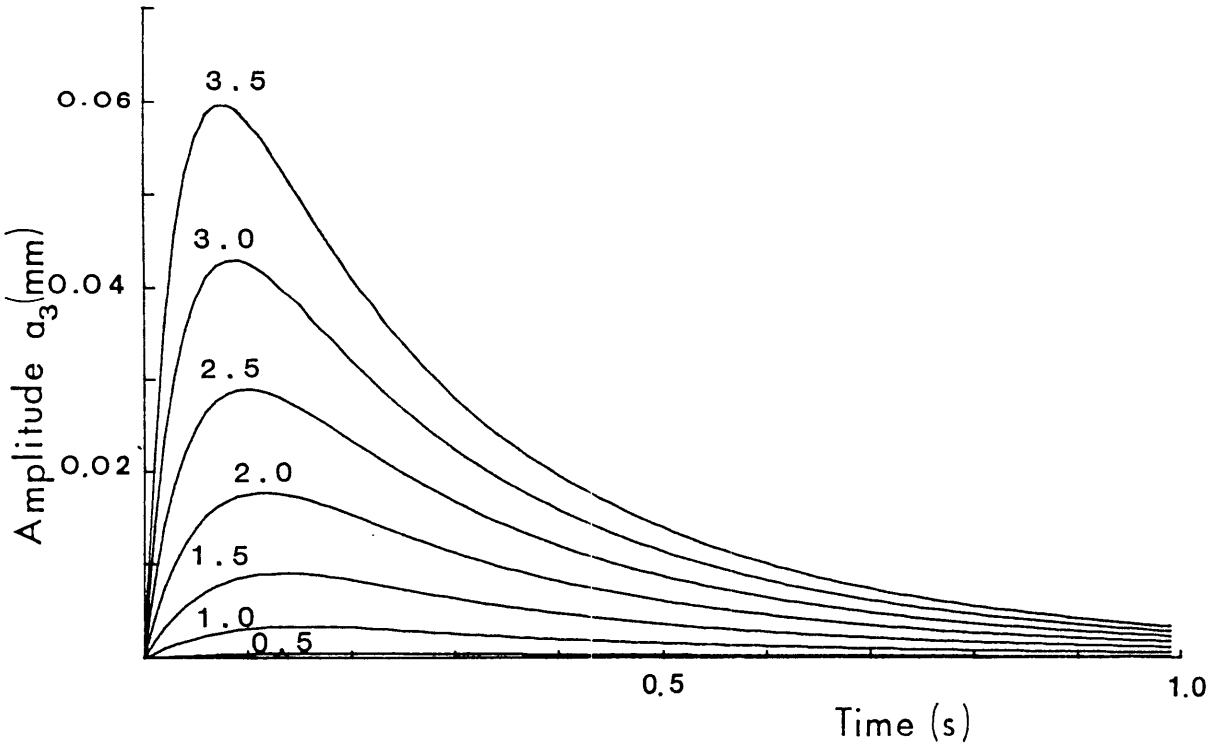

Figure 3.11: Calculated growth and decay of the third mode of the string, plucked at a node for that mode, for first mode amplitudes ranging from 0.5 to 3.5mm (shown as a parameter).

are of the right order in each case, and these amplitudes increase with the amplitude of the exciting fundamental with something close to the observed slope. More specifically, the calculated slope for $\log a_2$ against $\log a_1^0$ is about 1.6 and for $\log a_3$ against $\log a_1^0$ is about 2.2. The general slope for the experimental curves is in each case rather less than this. The calculated times to reach maximum amplitude are similarly of the observed order of magnitude but are significantly too small at small pluck amplitudes and show much too little variation with amplitude.

3.11 Discussion

It is quite apparent that while the theory can account for the observed phenomena in a general way it is only in semi-quantitative agreement with experiment. The most likely explanation for the residual disagreements is the failure of our experimental set-up to provide an adequate approximation to the idealized situation assumed for the theoretical analysis. This applies in particular to the behaviour of the bridge admittance. It seems unlikely that the higher order nonlinear terms omitted from the analysis could be large enough to influence the calculated results significantly although a more careful treatment of mode self-interaction and its associated frequency shifts may be necessary.

As a final observation we remark that, when there is appreciable inharmonicity in the string mode frequencies, whether from string stiffness or the compexity of the bridge admittance or other causes, it is possible to have much more complex behaviour than we have studied here. This can be seen explicitly in the case of mode 3 which, from (3.23) or (3.30) can be driven by mode 1 at a frequency $3\omega_1$ or by modes 1 and 2 at a frequency $2\omega_2 - \omega_1$. If these frequencies are not the same then beatlike behaviour ensues. This was easily observed in our mode 3 experiment by fixing a mass of a few hundredths of a gram to the midpoint of the string so as to lower the frequency of mode 1 while leaving mode 2 frequency unchanged (Fig. 3.12). The nonlinearities we have discussed also serve to couple in the same ways the modes that are actually excited on the string, so that they exchange energy and, if they are not ideally harmonic, fluctuate in amplitude.

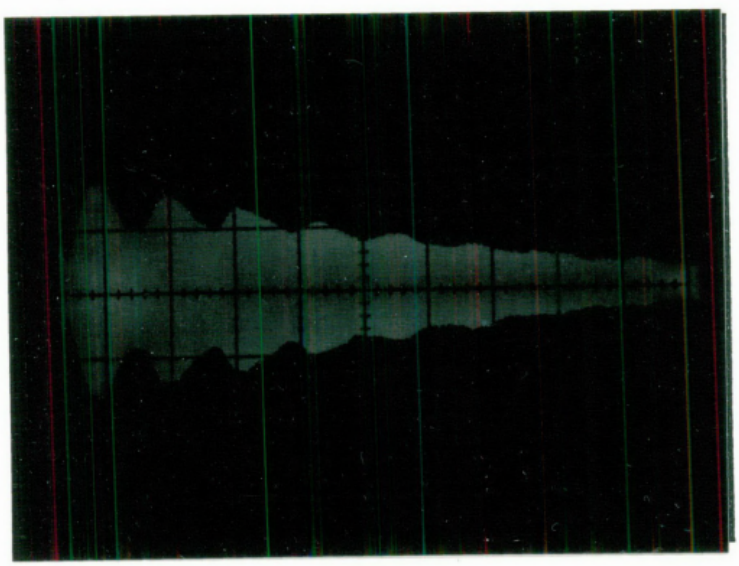

Figure 3.12: Oscilloscope record of the beatlike behaviour of mode 3 observed when a mass was attatched to the midpoint of the string so as to lower the frequency of mode 1 whilst leaving mode 2 unchanged.

3.12 Conclusions.

We have examined theoretically the nonlinear generation of missing modes on vibrating strings and have confirmed the predictions at least semi-quantitatively by experiment. The phenomenon has been shown to be confined to situations in which at least one of the bridges supporting the string has a nonzero mechanical admittance. This is of course the situation of practical importance in musical instruments.

Two different situations emerged from the analysis. If the nonrigid bridge has zero admittance parallel to the string length and if the string is fixed simply to it, then the only nonlinear process tending to mix modes or to generate missing modes is of third order. On the other hand, if the bridge is a nonrigid support over which the string passes at an angle, as in many musical instruments, then there is an additional second-order nonlinearity which provides driving forces at frequencies that are twice those of any mode present on the string.

These nonlinearities, as well as generating appreciable amplitudes for modes not initially excited on the string also serve to couple modes that are excited. In the practically important case in which mode frequencies are not in exact harmonic relationship, these couplings contribute fluctuations in the amplitudes of all the modes, which undoubtedly influences to some extent the auditory perception of the sound produced.

GLOSSARY OF SYMBOLS COMMONLY USED IN CHAPTERS 4 AND 5 FOR THE BAR.

x	position along the straight section of bar AB
y	position along the kinked section of bar BC
t	time
$\xi(x,t)$	transverse displacement of AB
z_1	transverse displacement of AB at bend
$\zeta(y,t)$	transverse displacement of BC
z_2	transverse displacement of BC at bend
$u(t)$	temporal component of normal mode over entire length of bar
$\psi(x)$	spatial component of normal mode over entire length of bar
a	amplitude
θ	phase angle
ω	radial frequency
ν	frequency
T_1	tension along AB
T_2	tension along BC
M	bending moment at bend
F	shearing force at bend
E	Young's modulus
S	cross-sectional area
ρ	mass per unit volume
L	length of AB
l	length of BC
κ	radius of gyration
ϕ	angle between AB and BC
α_n	$\left[\frac{\omega_n^2 \rho}{E\kappa^2}\right]^{\frac{1}{4}}$
Δ	change in length of AB
δ	change in length of BC
ξ'	nonlinear component of ξ
ζ'	nonlinear component of ζ
D	damping

τ	decay constant
β	mode coupling coefficient

Chapter 4

Review of the bar.

In mechanical terms there is really no sharp distinction between what is meant by a bar and what is meant by a string. In general, we refer to the restoring force acting on the system under motion to describe the difference: tension is more important in the case of the string and stiffness is more important for the case of the bar. There are, of course, an infinite number of intermediate cases from stiff strings to bars under tension where both stiffness and tension play a part. We shall be considering a bar under tension.

As with the string considered in chapters 2 and 3, the linear vibrational behaviour of a bar is well understood, although the analysis is far more complex for a bar than for an ideal string. However, since the linear analysis for the bar is somewhat less common than that for the string, it is perhaps worthwhile to briefly summarize it before proceeding to the nonlinear analysis. We shall follow the analysis given by Morse (1948) in doing this. It is

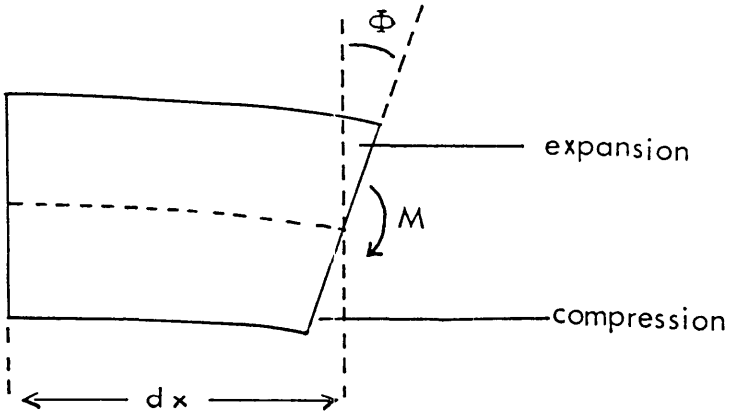

Figure 4.1: Bent element of bar acted upon by a moment M (from Morse 1948).

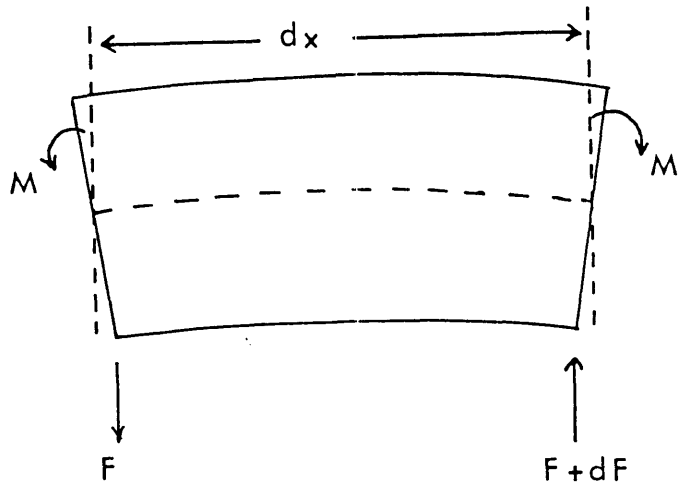

Figure 4.2: Bending moments and shearing forces to balance (from Morse 1948).

important to note however, that the notation we shall use for the analysis of the bar in this and the following chapter should not be compared with the notation used earlier for the string and that a fresh glossary of symbols has been compiled at the start of this chapter.

Consider a bar with uniform cross-section symmetric about a central plane and of length l and cross-sectional area S. When the bar is bent as indicated in Fig. 4.1, the lower part is compressed and the upper part is stretched. By considering the bar as a bundle of fibres and finding the bending moment required to bend each fibre by the angle Φ in the length dx (Fig. 4.2) then we quite easily deduce the total bending moment of the bar to be

$$M = \frac{E\Phi S\kappa^2}{dx} \tag{4.1}$$

where E is the Young's Modulus of the bar material and κ is the radius of gyration of the cross section. If the rod does not bend much then Φ may be written as

$$\Phi = -dx\left(\frac{\partial^2\xi}{\partial x^2}\right) \tag{4.2}$$

where ξ is the normal displacement of the bar, and (4.1) reduces to

$$M = -ES\kappa^2\left(\frac{\partial^2\xi}{\partial x^2}\right). \tag{4.3}$$

We can clearly see therefore that the bending moment is a function of the distance from one end of the bar. Thus we must balance the moments acting on the two ends of a bar element by a shearing force F (Fig. 4.2) leading to

$$F = \frac{\partial M}{\partial x} = -ES\kappa^2\left(\frac{\partial^3\xi}{\partial x^3}\right). \tag{4.4}$$

The shearing force too, is a function of x so that the net force acting on the element of bar may be written

$$dF = \left(\frac{\partial F}{\partial x}\right) dx \tag{4.5}$$

and this must equal the elements mass times its acceleration so that we obtain

$$\rho \frac{\partial^2 \xi}{\partial t^2} = -E\kappa^2 \frac{\partial^4 \xi}{\partial x^4}. \tag{4.6}$$

As a first step towards obtaining a solution of (4.6) we assume that it may be solved by separation of variables so that

$$\xi = v(x)\exp(i2\pi\nu t) \quad . \tag{4.7}$$

The general solution is then

$$\xi = [a\cos(2\pi\mu x) + b\cosh(2\pi\mu x) + c\sin(2\pi\mu x) + d\sinh(2\pi\mu x)]\exp(i2\pi\nu t) \tag{4.8}$$

where

$$\mu = \left[\frac{\nu^2\rho}{4\pi^2 E\kappa^2}\right]^{\frac{1}{4}} \tag{4.9}$$

and a, b, c, d are arbitrary constants.

This result leads to an important difference between the transverse vibration on a string and that of a bar. We can see from the above that the phase velocity, which is equal to $\frac{\nu}{\mu}$, and is independent of ν for a string, becomes

$$u' = \left[\frac{4\pi^2 E\kappa^2}{\rho}\right]^{\frac{1}{2}} \nu^{\frac{1}{2}} \tag{4.10}$$

for a bar. That is, it is dependent on the frequency of oscillation of the bar.

We now have the general solution for the transverse motion of a bar and require only the introduction of boundary conditions to calculate the set of allowed frequencies for any particular case. We shall not go into this here, but in chapter 5 we shall be investigating more thoroughly the linear analysis of a kinked bar and its allowed frequencies.

Up till this point we have assumed our bar to be ideal in as much as it has stiffness but no tension. To be more realistic then, requires the combination of the equations of motion for an ideal string and an ideal bar so that the intermediate case of a bar under tension T (or similarly of a stiff string) has the equation of motion

$$\rho \frac{\partial^2 \xi}{\partial t^2} = -E\kappa^2 \frac{\partial^4 \xi}{\partial x^4} + \frac{T}{S}\frac{\partial^2 \xi}{\partial x^2} \quad . \tag{4.11}$$

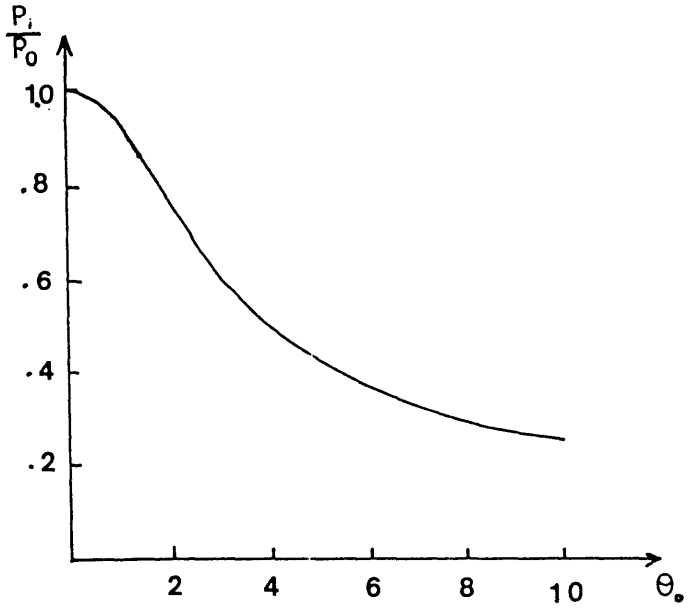

Figure 4.3: The ratio of nonlinear period over linear period, $\frac{P}{P_0}$, plotted against initial deflection angle θ_0. It can be seen that the classical theory is correct only for vanishing θ_0.(From Eringen 1951).

The general solution to this still has the form (4.7) but now

$$\mu^2 = \frac{-T}{8\pi^2 E S \kappa^2} + \left[\frac{T}{8\pi^2 \mathbf{E} S \kappa^2} + \frac{\nu^2 \rho}{4\pi^2 \mathbf{E} \kappa^2} \right]^{\frac{1}{2}} \tag{4.12}$$

which clearly reduces to (4.9) when $T = 0$.

The major cause of nonlinearity in the motion of a straight bar is similar to that for the string in that it is a result of an axial force induced in it by its vibrations when it is restrained in such a way that its ends are a fixed distance apart.

Eringen (1951) gives a detailed analysis of the vibration of straight bars, starting from first principles and without the linear assumption that the deflection is small and inextensional and so including on the bar, tension as a function of displacement amplitude. Solving for the particular case of a bar with hinged ends, he obtains the result shown in Fig. 4.3 where the nonlinear period over the linear period $\frac{P}{P_0}$ is plotted against the initial deflection angle θ_0 . Quite obviously the classical theory ($P_0 = P$)is correct only for vanishing θ_0 and the results show the "hardening" behaviour with increase in amplitude. Further documentation of this behaviour (eg:Eisley, 1964 and Srinivasan, 1966) has meant that the nonlinearity is well established and understood for any flat bar with immovable supports.

Prathap and Pandalai (1978) examine the vibration of bars with an initial curvature and show them to have a rather more complicated behaviour that changes from a hardening to a softening type depending on the amount of curvature and the initial amplitude of vibration.

There is, however, very little in the published analyses on nonlinear vibrations of bars that has relevance to our problem. In our case the boundary conditions are rather different, as seen in Fig. 4.4. The bar is symmetrically kinked and it is the behaviour around the kinks due to the motion of the bar that actually produces the nonlinear forces we shall be investigating. The analysis involves looking at the effects of these nonlinear forces on the linear modes of the bar. The kinks prove to be essential to the process.

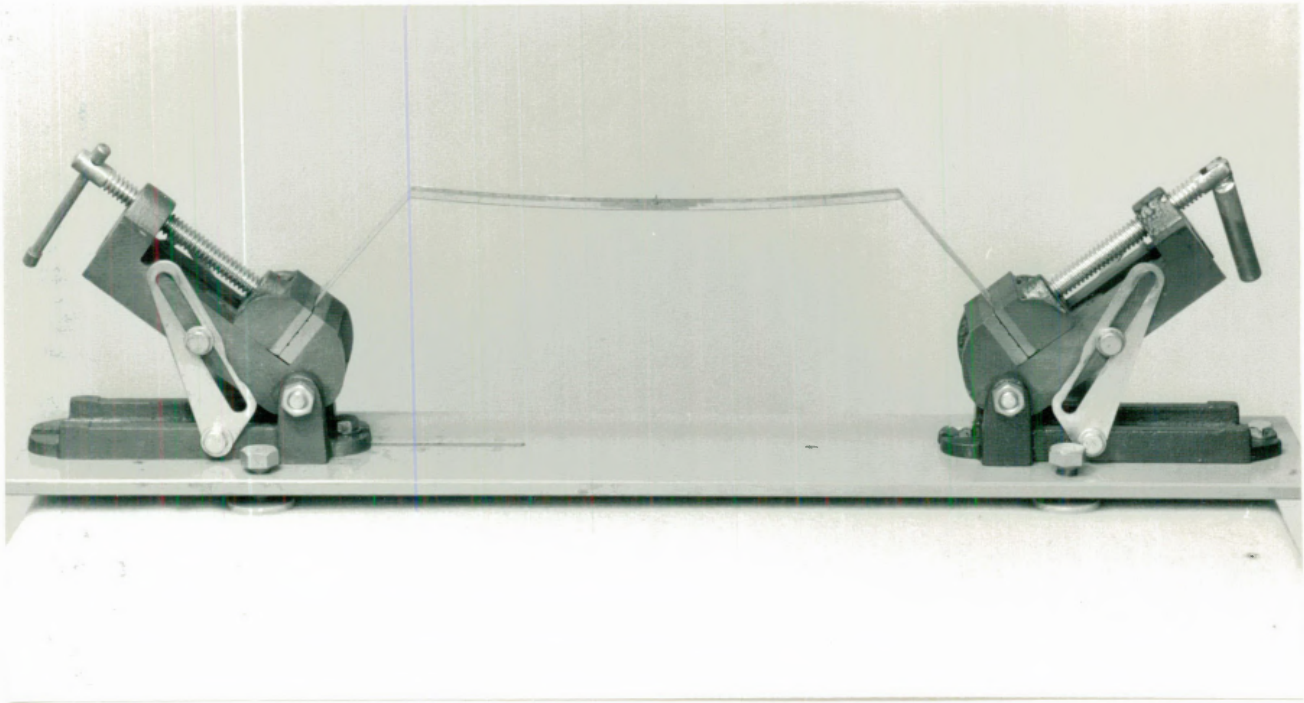

Figure 4.4: Photograph of the symetrically kinked clamped bar to be considered in the following chapter.